Using the intrinsic growth rate of the mosquito population improves spatio-temporal dengue risk estimation

Luigi Sedda, Benjamín M. Taylor, Alvaro E. Eiras, Joao Trindade Marques, Rod J. Dillon

▶ **To cite this version:**

Luigi Sedda, Benjamín M. Taylor, Alvaro E. Eiras, Joao Trindade Marques, Rod J. Dillon. Using the intrinsic growth rate of the mosquito population improves spatio-temporal dengue risk estimation. Acta Tropica, 2020, 208, pp.105519. ⟨10.1016/j.actatropica.2020.105519⟩. ⟨hal-02917265⟩

HAL Id: hal-02917265

https://hal.science/hal-02917265v1

Submitted on 18 Aug 2020

HAL is a multi-disciplinary open access archive for the deposit and dissemination of scientific research documents, whether they are published or not. The documents may come from teaching and research institutions in France or abroad, or from public or private research centers.

L'archive ouverte pluridisciplinaire **HAL**, est destinée au dépôt et à la diffusion de documents scientifiques de niveau recherche, publiés ou non, émanant des établissements d'enseignement et de recherche français ou étrangers, des laboratoires publics ou privés.

HAL Authorization

The use of the intrinsic growth rate of mosquito population improves spatio-temporal Dengue risk estimation.

Luigi Sedda[1,*], Benjamín M. Taylor[2], Alvaro E. Eiras[3], João Trindade Marques[4,5] and Rod J. Dillon[6]

[1]Lancaster Medical School, Furness Building, Lancaster University, Lancaster, LA1 4YG, UK

[2]Centre for Health Informatics, Computing, and Statistics (CHICAS), Lancaster Medical School, Furness Building, Lancaster University, Lancaster, LA1 4YG, UK

[3]Department of Parasitology, Instituto de Ciências Biológicas, Universidade Federal de Minas Gerais, Belo Horizonte, Minas Gerais, CEP 30270-901, Brazil

[4]Department of Biochemistry and Immunology, Instituto de Ciências Biológicas, Universidade Federal de Minas Gerais, Belo Horizonte, Minas Gerais, CEP 30270-901, Brazil

[5]Institut de biologie moléculaire et cellulaire, Université de Strasbourg, 67084 Strasbourrg, France

[6]Biomedical and Life Sciences, Furness Building, Lancaster University, Lancaster, LA1 4YG, UK

* Corresponding author:

Email: l.sedda@lancaster.ac.uk

Abstract

Understanding geographic population dynamics of mosquitoes is an essential requirement for estimating the risk of mosquito-borne disease transmission and geographically targeted interventions (precision public health). However, the use of population dynamics measures as predictors in spatio-temporal point process has not been investigated before. In this work we compared the model fitting statistics of four spatio-temporal log-Gaussian Cox models: (i) with no predictors; (ii) mosquito abundance as predictor; (iii) intrinsic growth rate as predictor; (iv) intrinsic growth rate and density of mosquitoes as predictors. This analysis is based on mosquito *Aedes aegypti* surveillance and human dengue data obtained from the urban area of Caratinga, Brazil. We used a statistical Moran Curve approach to estimate the intrinsic growth rate and a zero inflated Poisson kriging model for estimate mosquito abundance at dengue cases locations. The incidence of dengue cases were positively associated with mosquito intrinsic growth rate, which model outperformed (in terms of predictive accuracy) the abundance and the null models (which include only the spatio-temporal random effect but no predictors). In the light of these results we suggest that the intrinsic growth rate should be investigated further as potential tool for predicting the risk of dengue transmission and targeting health interventions for vector-borne diseases.

Keywords

Moran curve, Ricker model, density dependent and independent mortalities, log-Gaussian cox process, dengue, *Aedes aegypti*.

Introduction

Understanding mosquito population dynamics, the regulation of insect populations in different environments, is fundamental to develop models for estimating the entomological risk of mosquito-borne disease transmission that can be used for effective mosquito surveillance and control, e.g. precision public health. Current indexes (e.g. Breteau, number of disease cases surpassing a pre-defined threshold) are efficient only when mosquito infestation is already happening, or when multiple indexes are combined (Vargas, Kawa et al. 2015). Despite the variety of methods and their availability (Tonnang, Hervé et al. 2017), current risk assessment models for vector-borne diseases are still often based on static species occurrence models, e.g. spatialization of presence/absence or count abundance, which lack information about insect population dynamics, i.e. mortality, fertility and density dependence effects (see for example the recommendations from (Ehrlen and Morris 2015)). When longitudinal data is available, dynamic models can provide essential information for vector-borne disease risk management (Cromwell, Stoddard et al. 2017, Tonnang, Hervé et al. 2017).

The dynamicity of a mosquito population depends on its behaviour (i.e. timing of diapause, host seeking) and the dependence of its demographic parameters from environmental changes. Mosquito populations can respond rapidly (from hours to days) to meteorological changes (Parham, Pople et al. 2012, Armbruster 2016), determining abrupt variations in population abundance (Jian, Silvestri et al. 2014), especially in areas where rainfall and temperature are strongly seasonal (Jian, Silvestri et al. 2014). Vector mortality/survival is one of the parameters, linked to population dynamics, used to describe disease transmission (Brady, Golding et al. 2014). Vector mortality depends on density dependent mortality (DD), which for mosquitoes has been suggested as one of the main parameters affecting vector control measures (Legros, Otero et al. 2016) at different insect life stages particularly the

aquatic stage (Phuc, Andreasen et al. 2007). DD is modulated by social and trophic interactions, such as cannibalism, competition, crowding, cooperation, diseases, herbivory, mutualism, parasitism, parasitoidism, predation, and reproductive behaviour (Gerber, McCallum et al. 2005, Herrando-Pérez, Delean et al. 2012).

The aim of the study is to evaluate if the spatio-temporal variation in the intrinsic growth rate is better associated to the incidence of dengue cases than spatio-temporal mosquito abundance. The geographic association between dengue cases and mosquito intrinsic growth rate and abundance is evaluated for a Dengue endemic area in Brazil. The advantage in the use of intrinsic growth rate is that its estimation requires abundance data only when compared to other indexes (reproductive number, R0, and vectorial capacity (Reiner, Perkins et al. 2013)).

Dengue is the second most important vector-borne disease worldwide with 2.5 billion people at risk (World Health Organization 2014). Dengue and other arboviral diseases (Zika and chikungunya) lack efficient vaccines, are transmitted by the same *Aedes* vectors, and their control still relies on preventing contact between vector and humans (World Health Organization 2009). The dengue cycle involves mosquitoes and humans, although limited virus circulation in other vertebrate hosts has also been reported (Diallo, Ba et al. 2003, de Thoisy, Lacoste et al. 2009). According to the World Health Organization, Brazil currently occupies the first place in the ranking of reported dengue cases in the world with incidence rates increasing since 2004 (Fares, Souza et al. 2015) with poorly understood efficacy of its control (Bowman, Donegan et al. 2016).

Aedes aegypti (L.) (Diptera: Culicidae) mosquito is responsible for the urban transmission of the dengue virus (Kraemer, Sinka et al. 2015). Its populations are considered to be regulated

by a strong density dependent mortality (Robert, Okamoto et al. 2014). *Ae. aegypti* is highly anthropophilic, water containers or drains associated with human habitation are the principal breeding habitat. These mosquitoes lay eggs on the inner wall of water filled containers. Female *Ae. aegypti* feed almost exclusively on humans in daylight hours and typically rest indoors. This mosquito species is very mobile, although the flight range during its life span is no more than 1km (Sarfraz, Tripathi et al. 2014) and the majority of the population stays within 200m (Sarfraz, Tripathi et al. 2012). Oviposition and aquatic stages of *Ae. aegypti* are thought to be regulated by density dependence (Lana, Carneiro et al. 2014), while adults may be regulated mainly by density independent events, with few cases involving density dependence mortality.

This work is composed of two parts. Firstly, we used a process-based compartmental framework (which assumes independence between some of the population parameters) to estimate the: unlimited growth λ_0, from Equation 3; the density independent mortality, *DI*, from equation 4; the potential total mortality, *DT*, from equation 5; the density dependent parameters, *d* and α, from equation 6; the density dependence, *DD*, from equation 8; and the intrinsic growth, *IGR*, rate from equation 10. Secondly, we evaluated whether the intrinsic growth rate is significantly associated with dengue spatio-temporal incidence and how it compares with a mosquito abundance model and a null model (intercept+spatio-temporal random effect). This section of the analysis is based on a spatio-temporal log-Gaussian Cox model (Taylor, Andrade-Pacheco et al. 2018).

Materials

Study area

The study was conducted in the municipality of Caratinga located in the eastern region of Minas Gerais state, Southeastern Brazil (19° 47′ 24″ S, 42° 08′ 20″ W) (Figure 1). The study area had a total territorial extension of 12 km^2 with approximately 90,000 inhabitants. Atlantic forest is the biome of the municipality with 21ºC median annual temperature and 80% humidity (data from the Brazilian Ministry of Agriculture - INMET) (Ministério da Agricultura 2015). The city is classified as a dengue endemic area, it had 1274, 91, 409 and 51 confirmed dengue cases from 2007 to 2010 respectively (data from the Brazilian Ministry of Health - SINAN) (Saúde 2015) showing a large fluctuation in dengue cases despite dengue awareness campaigns and control of dengue breeding sites (for example in 2012 there have been 55 dengue cases while in 2013 721 cases were recorded). These fluctuations are typical for infectious diseases such as dengue, where the spatial variability of the four serotypes and the susceptibility of human populations to primary and secondary infections changes over time (for Brazil see (Rodriguez-Barraquer, Cordeiro et al. 2011, Cortes, Turchi Martelli et al. 2018)).

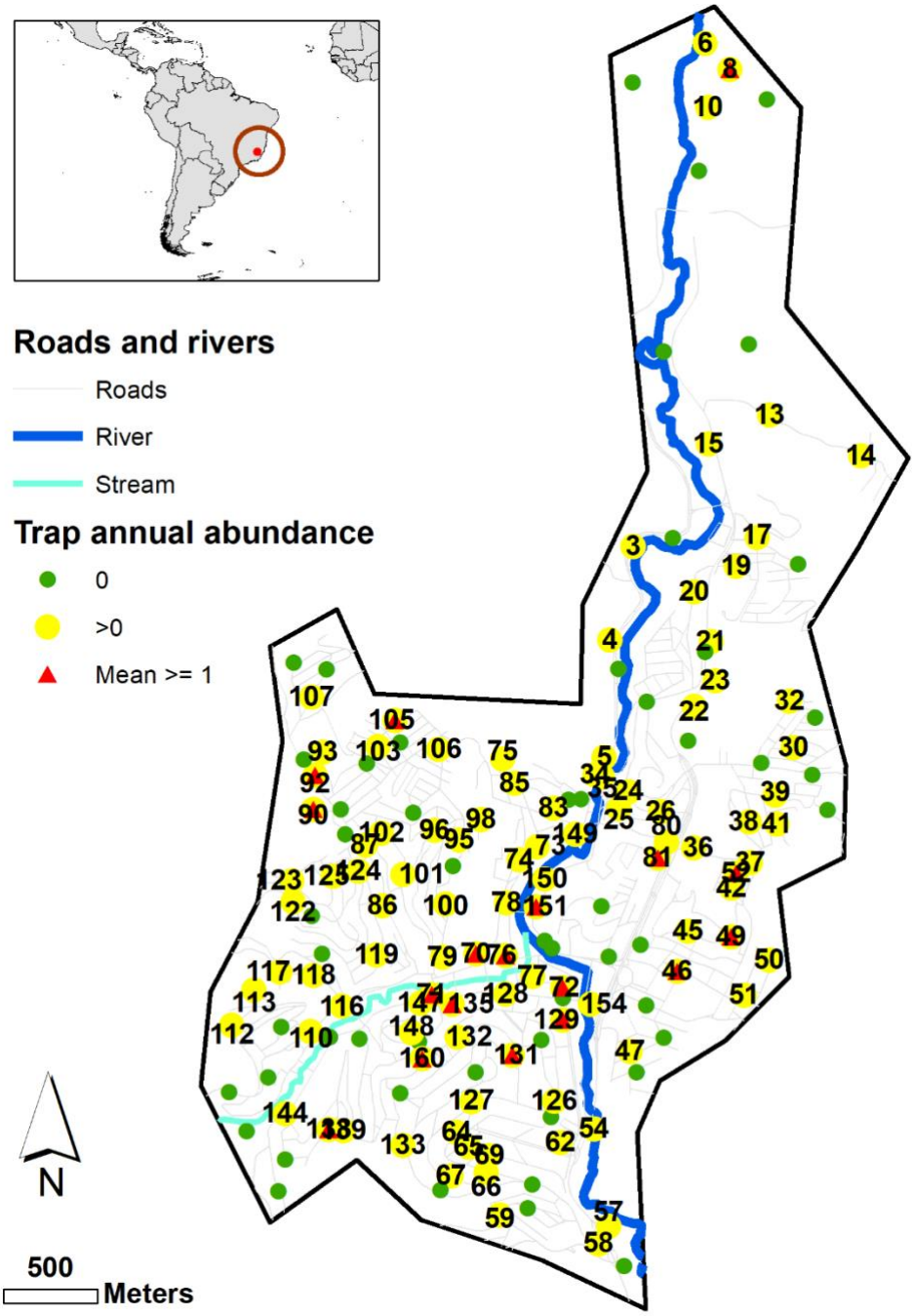

Figure 1. Study area in the municipality of Caratinga, Minas Gerais, Brazil. Location of the mosquito traps without (green) and with (yellow) catches of *Ae. aegypti* mosquito during the sampling period (2010-2011). Red triangles show those traps with average annual catches of 1 or more mosquitoes. Traps highlighted with identificatory number. Numeric monthly catches at each trap are shown in supplementary table ST1. Roads, streams and rivers obtained from OpenStreetMap https://www.openstreetmap.org under CC BY-SA licence. World countries map from Natural Earth, CC BY-SA @ naturalearthdata.com.

Sampling design and mosquito collection data

The data was obtained using the Intelligent Aedes Monitoring System (MI-Aedes) (Ecovec, Belo Horizonte, Brazil) adopted by the Caratinga municipality (Álvaro Eduardo Eiras 2009), which deployed mosquito sticky traps known as MosquiTRAP (Favaro, Dibo et al. 2006, Pepin, Marques-Toledo et al. 2013) baited with synthetic oviposition attractant to capture gravid *Aedes* mosquitoes. 158 traps were placed at a maximum of 300m apart following a 300 m by 300 m grid design as described in a previous work (Sedda, Vilela et al. 2018). However, in practice the 300 m design was rarely achieved due to the lack of permission to locate the traps in the back or front yard of private properties and distance between traps ranged from 40 to 300m (Figure 1).

Collection of the mosquitoes started in August 2010 and was completed in July 2011. Traps were inspected once a week and each captured mosquito was identified by species and sex (Consoli and Oliveira 1994).

Environmental correlates

The environmental variables used in the proposed framework were the air temperature (AT), relative humidity (RH), wet bulb temperature (WT) and atmospheric pressure (AP) as measured every 6 hours by the Brazilian Instituto National de Meteorologia (http://www.inmet.gov.br) meteorological station located in the North border of Caratinga at 600 m of elevation. AT, RH and WT were the variables most significantly associated with mosquito mortality, while AT, RH, WT and AP with mosquito abundance (see discussions). Other variables such as haziness, wind speed and wind direction, were not significant. Due to the small dimension of the area (6 x 3 km) and distances between traps, we considered only the values from the above meteorological station. However, averages for the meteorological

variables at each trap differed since averages are based on the day of trap inspection (see methods).

Dengue cases

During the mosquito sampling campaign, 44 dengue cases were confirmed with onset of symptoms between November 2010 and July 2011. DENV1 and DENV3 were the most common dengue serotypes, while DENV2 was confirmed in only one patient. Month of symptom onset and geographic coordinates were used for this analysis, i.e. IGR and mosquito abundance were extracted at the month of onset of symptoms and within 100 m from the home address (see methods). Home address reported to health authorities were anonymized. Unlinked anonymous testing of human blood samples (where the term unlinked refer to blood samples obtained from tests not exclusively for dengue) was approved by the ethics committee in research (COEP) of Universidade Federal de Minas Gerais (number 415/04). Use of this secondary data was also approved by the Faculty of Health and Medicine Research Ethics Committee at Lancaster University (FHMREC18067).

Development of Statistical Methods

The statistical analysis was performed on the monthly sum of catches of female adult *Ae. aegypti* for each trap. AT, RH, WB and AP were monthly averaged for a month before the day of trap inspection (i.e. for the 14th October inspection, AT, RH, WB and AP were individually averaged from 14th September to 13th of October). Other monthly temporal lags (i.e. 2 and 3 months before trap inspection) were tested but their coefficients were not statistically significant (see supplementary table ST2). Analyses were carried out in R-cran software (Chambers 2008).

Statistical Moran curve approach

The Moran curve approach accounts for unlimited growth rate (λ_0) which modulates the density independent mortality (*DI*) and the density dependent mortality (DD). The latter can be parameterised by its intensity (α) and population density at which density dependent mortality starts (d) (Figure 2). All these components are estimated in order to provide a measure of point IGR as described in the following sections.

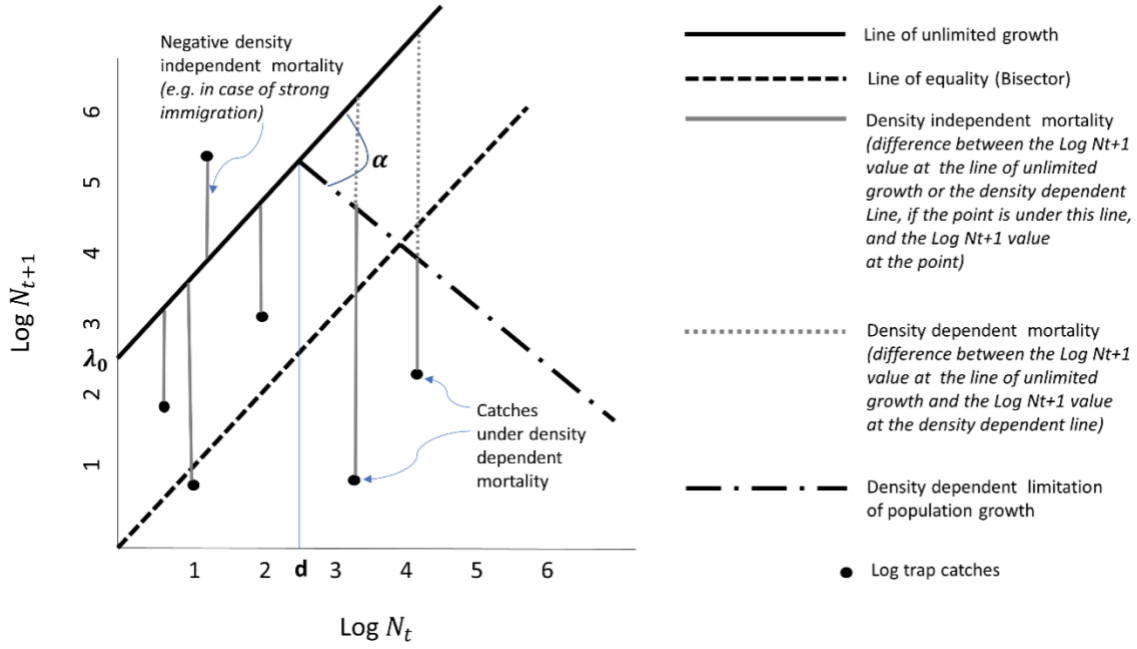

Figure 2. Graphical explanation of the Moran curve parameters. The density independent mortality at a mosquito log density point (log trap catches) is the difference of the log density values between the line of unlimited growth (which intercept is the unlimited growth λ_0) and the log density point; while the density dependent mortality is the difference between the log density values between the line of unlimited growth and the line of density dependent limitation of population growth. When the density dependence is acting (densities > *d* otherwise density dependence is 0) then the density independent mortality is the difference of log density values between the line of density dependent limitation of

population growth and the point. The intensity of density dependent mortality is represented by the slope α.

Step 1. Unlimited growth calculation

The Ricker model (Turchin 2003) describes the species abundance or density at time t+1:

$$N_{t+1} = \lambda_0 N_t exp(\alpha N_t) \quad [1]$$

where t is the time step, α is the parameter controlling the density dependence, and λ_0 is the unlimited growth. α implies regulation when its value is below 0 while for $ln(\lambda_0)$<2, the population is considered stable (Hoshi, Imanishi et al. 2017). In statistical terms, density dependence is equivalent to the partial autocorrelation between two consecutive (in time) mosquito densities (Jian, Silvestri et al. 2014). Equation [1] can be fitted using a negative binomial distribution with over-dispersion parameter (Royle 2004), k:

$$N_{t+1} \sim NegBin(mean = \lambda_0 N_t exp(\alpha N_t), overdispersion = k) \quad [2]$$

This model implies stochasticity in individuals independent of their density. In order to estimate the maximum unlimited growth λ_0 (as defined by the Moran curve approach (Rogers 1979), see Figure 2 as graphical reference for all the parameters), we omitted the density dependent term from [2] and estimated λ_0 from:

$$N_{t+1} \sim NegBin(mean = \lambda_0 N_t, overdispersion = k) \quad [3]$$

via iteratively reweighted least squares (Hastie 2017).

Step 2. Moran Curve density independence mortality

The $\widehat{\lambda_0}$ estimated from Equation 3, can be plugged in Equation 4 to estimate the density independent mortality (*DI*) at each trap, *s*, and time, *t*:

$$\log(DI_{t,s}) = \widehat{\lambda_0} + \log(N_{t,s}) - \log(N_{t+1,s}) \quad [4]$$

Step 3. Moran curve density dependence mortality

Let's first define *DT* (assimilable to the potential total mortality or k-value (Varley and Gradwell 1960)) as:

$$DT_{t,s} = log(N_{t,s} + \widehat{\lambda_0}) \quad [5]$$

Once this quantity has been estimated from equation 5 (using $\widehat{\lambda_0}$ from Equation 3 and $N_{t,s}$ from the data), the population size at which the density dependent mortality starts, *d*, and the intensity of density dependence, α, can be estimated by assuming *DT* normally distributed and modelled via generalized linear mixed model (using an iteratively reweighted least squares fitting method):

$$\log(DT_{t,s}) \sim N(d + \beta\mathbf{X} + \alpha \ \log(N_{t,s}) + \varphi\mathbf{R}, \sigma^2) \quad [6]$$

where σ^2 is the constant scale parameter; **X** is a matrix of scaled (by removing the mean and dividing by the standard deviation) environmental covariates (AT, RH and WT) with regression coefficients β; **R** is a the random effect (trap ID); and φ the coefficient for the random effect. Assuming the density dependence as a switch process (absent when densities are lower than *d*) is inaccurate since density dependence is always present, although at very low intensities for small population sizes (Sedda, Mweempwa et al. 2014).

α is commonly regarded as the intensity of the density dependent mortality. Expressing α in degrees clockwise from the unlimited growth line (Figure 2):

$$\alpha\ (degrees) = 90 - (\tan^{-1}(\alpha))\left(\frac{180}{\pi}\right) \quad [7]$$

and following the interpretation of the slope from (Varley, Gradwell et al. 1973), a population can be classified as:

a) undercompensating, if α is lower than 45 degrees (0<b<1 in (Varley, Gradwell et al. 1973))

b) exact compensating, if α is equal to 45 degrees (b=1 in (Varley, Gradwell et al. 1973))

c) overcompensating, if α is larger than 45 degrees (b>1 in (Varley, Gradwell et al. 1973))

The adjustment of 90 degrees is due to the rotation of the axis during the modelling of d and α (see (Varley, Gradwell et al. 1973) pages 22 and 23).

Monthly density dependence mortality values at each location are produced by the following mathematical system of equations (symbols as in Figure 2):

$$if\ \log(N_{t,s}) \leq d$$

$$\log(\widehat{DD}_{t,s}) = 0$$

[8]

$$else$$

$$\log(\widehat{DD}_{t,s}) = (\log(N_{t,s}) - d\ \ )(1 + \tan(\alpha))$$

Step 4. Obtaining intrinsic growth rate of mosquito population

In the last two steps we estimated the contribution of both density dependent and independent mortalities to changes in total generation mortality over several generations. It is important to specify that mortality (density dependent and independent) is used broadly in this context, and contains immigration and emigration processes. A strong immigration will therefore be characterized by a negative mortality (Figure 2). At equilibrium or stability point, the difference between unlimited growth and density independent mortality is thus accounted for by density dependent mortalities (e.g. competitors, predators or parasites). If inescapable density independent losses exceed unlimited growth rate, the population will be in continuous

decline until it becomes extinct. Such populations can persist in an area only if they are periodically 'topped up' from elsewhere by immigration. In this approach, the unlimited growth is usually assumed to be constant, this means that variations in unlimited growth are treated as variations in mortality; this is unlikely to be a serious problem because natural variations in unlimited growth are very much less than natural variations in mortality (Sedda, Mweempwa et al. 2014).

The adult population change in size between two consecutive time steps due to losses (mortality, emigration) and gains (fertility, immigration) (Herrando-Pérez, Delean et al. 2012) is called the intrinsic growth rate, IGR::

$$IGR = \widehat{\lambda_0} - \log(DI_{t,s}) - \log(DD_{t,s}) \quad [10]$$

with $\widehat{\lambda_0}$ from Equation 3, *DI* from Equation 4 and *DD* from Equation 8.

Step 5. Mosquito intrinsic growth rate and abundance mapping

Monthly mosquito intrinsic growth rate and abundance and their standard deviations at each point, *s*, and month, *t*, in a grid of 5 by 5m were estimated.

Mosquito abundance was modelled with a zero inflated Poisson regression (ZIP) spatio-temporal kriging. In practice the residuals from a zero inflated Poisson regression on mosquito abundance were mapped via spatio-temporal kriging. Abundance at each point in the grid was obtained by summing the predicted residuals (from the kriging) with the deterministic trend surface (from the ZIP). Following the notation in (Lambert 1992) and assuming the same model of Equation 1, the mosquito abundances *N* are independent with:

$$N_{t,s} \sim 0 \quad with\ probability\ p_{t,s}$$

$$N_{t,s} \sim Poisson(u_{t,s}) \quad with\ probability\ 1 - p_{t,s}$$

therefore when: [11]

$$N_{t,s} = 0 \quad the\ probability\ is \quad p_{t,s} + (1 - p_{t,s})e^{-u_{t,s}}$$

$$N_{t,s} = q \quad the\ probability\ is \left(1 - p_{t,s}\right)e^{-u_{t,s}} \frac{u_{t,s}^{q}}{q!}$$

with q=1,2,…, Q, and parameters for the log linear model defined as:

$$log(\mathbf{u}) = \boldsymbol{\beta_u}\mathbf{W}$$

[12]

$$log(\mathbf{p}) = \boldsymbol{\beta_p}\mathbf{B}$$

with **W** and **B** covariates for the Poisson mean (**u**) (which is the count model) and the probability of the perfect state (**p**) (which is the zero-inflation model) respectively. In this work we have chosen **W** as matrix of four covariates, three common to the Moran curve analysis (air temperature, relative humidity and wet bulb temperature) and one, atmospheric pressure added since improving the model fit. Matrix **B** is a column of traps ID. Using the same covariates in **W** for **B** or other covariates do not improve the model fit. In this mixture model, the counts are modelled with a Poisson distribution, while the zero-inflation used a binomial model. The analysis was run using the function zeroinfl in pscl R package (Zeileis, Kleiber et al. 2008).

Residuals from the ZIP model were mapped as spatial process $Z(t,s)$ with an ordinary spatio-temporal kriging:

$$Z(t,s) = \mu + e(t,s) \qquad [13]$$

where μ is the constant mean (assumed constant over the area), $\mathrm{E}\big(e(t,s)\big) = 0$ and covariance, $\mathrm{Cov}\big(e(t,s)\big) = V$. When V is known the best linear unbiased prediction of an unsampled location $Z(t_0,s_0)$ is

313 $$\widehat{Z(t_0,s_0)} = \mu + v_0^{'} V^{-1}(z(t,s) - \mu)$$

314 and: [14]

315 $$v_0 = \left(Cov\left(e(s_1,t_1), e(s_0,t_0)\right), \ldots, Cov\left(e(s_n,t_m), e(s_0,t_0)\right)\right)$$

316 where all the coupled locations are within a spatial distance ω and temporal distance ρ; the
317 covariance function (of a second order stationary process) is a separable double exponential
318 model:

319 $$Cov(\omega,\rho) = \gamma^2 exp\left\{-\frac{\Delta_s}{\omega} - \frac{\Delta_t}{\rho}\right\}$$ [15]

320 with spatial range ω , temporal range ρ, and the Euclidean distance Δ in space, *s*, and absolute
321 distance Δ in time, *t*, as indicated by the subscript; and with expectation $\mathbb{E}[e(s,t)] = -\frac{\gamma^2}{2}$ for
322 all *s* and *t*.

323 In practice, ω and ρ delimit the maximum spatial and temporal distances at which
324 autocorrelation (and therefore smoothness) exist between two locations.

325 The shape of the covariance $Cov(\omega,\rho)$, and the values of, ω, and ρ were selected based on
326 those minimizing the mean squared error. Uncertainty around these values is provided by
327 producing the covariance envelopes. These are calculated from a spatial permutation of the
328 data values at the trap spatial locations and by re-fitting the experimental covariance
329 (Equation 15). The number of permutations was 999 (Walker, Loftis et al. 1997).

330 The intrinsic growth rate from step 4 was mapped by employing the same ordinary spatio-
331 temporal kriging model and covariance (double exponential) described above (Equations 13,
332 14 and 15).

Monthly predictions and 12 months average are provided with standard errors obtained from the kriging variance. Spatio-temporal ordinary kriging was performed using the function krigeST from gstat package.

Testing the alternative

We compared our density dependence estimates with the negative binomial generalized linear model proposed by Chaves and colleagues (Chaves, Imanishi et al. 2015) to fit the environmental stochastic Ricker model:

$$N_{t+1} \sim NegBin(mean = \lambda_0 N_t exp(\alpha N_t + \beta \mathbf{X}_t), overdispersion = k) \quad [16]$$

This equation is one of the common approaches in modelling longitudinal data for species abundance. It allows for the estimation of unlimited growth and density dependence intensity in the presence of environmental factors. In order to account for random effects originated by repeated collections of mosquitoes from the same trap, we employed a negative binomial generalized mixed model (function glmer.nb in lme4 R package), with trap ID as random effect. In **X** we use the same covariates of Equation 6 (AT, RH and WB) with one month lag.

Comparing predictors for dengue cases model

We evaluated if any spatio-temporal association exists between the incidence of dengue cases and the mosquito intrinsic growth rate and abundance. To model dengue cases at the pixel level across our study region we assumed that the locations of the cases follow a spatiotemporal log-Gaussian Cox process (Taylor, Andrade-Pacheco et al. 2018, Taylor 2019). This model assumes the number of cases, Y(*s*; *t*) follows a Poisson distribution:

$$Y(s,t) = Poisson[M(s,t)] \quad [17]$$

$$logM(s,t) = \log\big(P(s,t)\big) + \beta X(s,t) + G(s,t)$$

where $P(s; t)$ is a known component of the intensity function (the 2010 number of people per grid-cell from WORLDPOP project (Tatem 2017), which is provided at a resolution of 3 arc seconds, meaning approximately 100m), $\mathbf{X}(s; t)$ is a vector of covariates (mosquito abundance and/or IGR), β is a vector of parameter effects to be estimated and $\mathbf{G}$ is a spatiotemporal Gaussian process where covariance is modelled as in Equation 15.

We used zero mean independent Gaussian priors for β with standard deviation 10_4. For $\log \gamma$, $\log \omega$ and $\log \rho$, we used independent Gaussian priors with respective means 0, log 100 and 0 and respective standard deviations 0.3, 0.3 and 1. Our prior for ω gives a range of up to around 400m, a value based on IGR and mosquito abundance modelling (Table 1 and 2). The parameter γ controls the variability in the latent spatial process, $\mathbf{G}$. We ran the MCMC algorithm for 3,000,000 iterations, using a burn-in of 100,000 iterations and retaining every 2,900th sample to give us a final sample of size 1000. We checked for convergence and good mixing of our chain by examining the trace plot for each parameter and we also used a plot of the log posterior density over the iterations as a global measure of convergence (Supplementary Figure S1). Computation for the main analysis in this paper took place on an NVIDIA Titan XP GPU with 3840 CUDA cores and 12GB GDDR5X RAM.

The four models evaluated here are with a null model with no $\mathbf{X}$ component; $\mathbf{X}$=IGR, $\mathbf{X}$=mosquito abundance, $\mathbf{X}$=IGR and mosquito abundance. Each model has an intercept term and a spatio-termporal Gaussian process (random effect).

To evaluate the predictive accuracy of these Bayesian hierarchical models we have used two information criteria: Deviance Information Criterion (DIC) and Watanabe-Akaike information criterion (WAIC) which penalise differently the log posterior predictive density. Both measures are designed for Bayesian analyses, however WAIC averages over the posterior distribution rather than conditioning on a point estimate as in DIC (Gelman, Hwang

et al. 2014). This translates in the fact that WAIC takes into account the predictions used for new data, while DIC takes into account the performance of the predictive density for predictions (Gelman, Hwang et al. 2014). As pointed out by (Vehtari, Gelman et al. 2016) "DIC can produce negative estimates of the effective number of parameters in a model and it is not defined for singular models. The WAIC is fully Bayesian in that it uses the entire posterior distribution, and it is asymptotically equal to Bayesian cross-validation. Unlike DIC, WAIC is invariant to parametrization and also works for singular models". However, WAIC often produces values with small differences between models with similar structure (see for example (Gelman, Hwang et al. 2014) and for an ecological application (Elderd)), therefore we have decided to report both WAIC and the DIC estimates in order to provide evidence of consensus between the two statistics and report a measure, the DIC, which is familiar among Bayesian ecologists.

Results

The majority of captured *Aedes* mosquitoes were female (95.9%) and belonging to *Ae. aegypti* (88%). The *Ae. aegypti* mosquito surveillance data was characterised by a large amount of zero catches (83% of the entire dataset). The non-zero range spans from 1 to 16 *Ae. aegypti*. The data is characterised by a strong seasonality with largest mosquito catches in the wet season (December to May with up to 110 *Ae. aegypti* total area catches) and lowest mosquito catches in the dry season (June to November, with maximum of 25 *Ae. aegypti* total area catches). See supplementary table ST1 for catches in individual traps. Finally 66% of the traps caught at least one *Ae. aegypti* mosquito during the surveillance campaign (traps indicated in yellow in Figure 1).

Moran curve estimated parameters

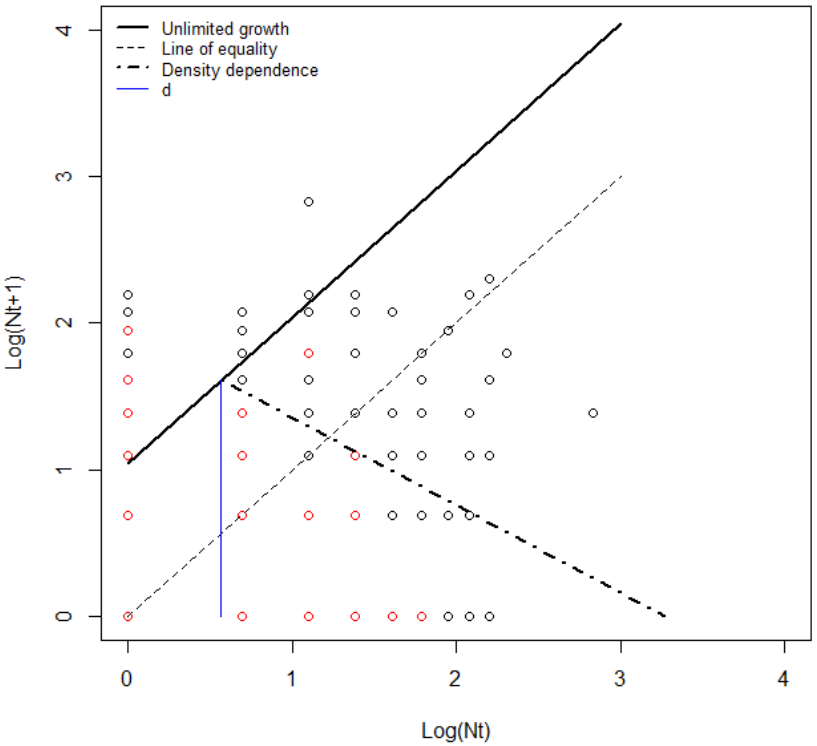

Figure 3. Plot of the estimated Moran Curve for *Ae. aegypti* caught in 158 traps in Caratinga. Points represent the log abundances (*N*) at time t (x-axis) and t+1 (y-axis). Red points are highly frequent abundance combinations (i.e. occurring more than 3 times). See Figure 2 for explanation of the lines.

Ae. aegypti population dynamic in terms of Moran curve parameters are presented in Table 1 and visualized in Figure 3. As per the original formalization of the Moran Curve (Rogers 1979), Figure 3 shows lines fitting the points and the mortalities. The lines were drawn based on the results from different models (Step 1 and 2). In Figure 3 the unlimited growth rate line has intercept λ_0 (obtained from Equation 3 (Royle 2004)) and slope of 45 degrees (i.e. population assumed with constant unlimited growth). This line does not overlay all the points (representing mosquito abundances). Points above this line may indicate the presence of

mosquito immigration (Sedda, Mweempwa et al. 2014), however given the heterogeneity in the number of mosquitoes captured per trap, large abundances may be due to natural variation within population and unable to be explained by a 12 months survey (see discussions). The density dependence starts at log abundance (*d*) of 0.58 with slope (α) of 56.3 degrees (both parameters obtained from Equation 6 assuming normal distribution for the mortality). Again, the density dependent line did not fit the points because it is modelled to fit the quantity DT (visually this would mean to rotate the unlimited growth rate as the y axis of a new plot). The slope is larger than 45 degrees indicating an overcompensating population (see Figure 2.9 in (Varley, Gradwell et al. 1973)). However, not all the traps show similar values. In fact some of the traps (supplementary table ST3) were under extreme overcompensation (slope larger than 90 degrees) while others undercompensated (slope lower than 45 degrees). Individual unlimited growth lines (supplementary table ST3) were generally below the one of the general model (69% of the traps) since a large proportion of traps are affected by a higher concentration of low mosquito abundances (the combination of zero catches at time t and t+1 are 661, e.g. 57% of the data points shown in Figure 3). Similarly, the density dependent line of the general model, which is affected by large abundances, is often above the individual trap density dependent line (61% of the traps). The average slope for individual traps (60 degrees) is close to the one of the general model (56 degrees).

Table 1 shows the estimated coefficients, envelopes and standard errors for the parameters of *Ae. aegypti* intrinsic growth rate framework. The estimated parameters for the exponential spatio-temporal covariance are a spatial range of 336m, and a temporal range of 6 months (Table 1), equivalent to the length of the seasons. The estimated nugget to sill ratio (a measure of explained spatial variance) is above 70% in both the spatial and temporal covariances demonstrating the presence of a strong spatial dependence (fitted by the double exponential function) and showing, once again, the importance of using spatially explicit

functions in modelling mosquito population dynamics (Hassell, Comins et al. 1991, Allen, Brewster et al. 2001, Cianci, Hartemink et al. 2015). The relatively short spatial range of the intrinsic growth rate (lower than 1 km when considering the envelopes) may indicate spatial fragmentation of mosquito-related local factors (breeding sites, humans and their settlements etc…). The covariates are statistically significant and coefficient signs are coherent with the biology of *Ae. aegypti* (see discussions) (Derrick and Bicks 1958, Li, Xu et al. 2019).

Table 1. Spatio-temporal Kriging and Moran curve parameters. Uncertainties provided as envelopes for the spatio-temporal covariance parameters, and as standard errors for the Moran curve parameters.. *Standardised so that the sum of the nugget and partial sill is equal to 1.

Parameters	**Value**	
Kriging model: Spatio-temporal covariance		**Envelopes**
ω, spatial range (m)	366	73,211
ρ, temporal range (months)	6.000	1,9
Spatial nugget*	0.169	0,0.51
Spatial partial sill*	0.831	0.5,1
Temporal nugget*	0.269	0,0.62
Temporal partial sill*	0.731	0.3,1
Moran curve model. Coefficients from Equation 6		**Standard errors**
Air temperature (scaled)	0.521	0.227
Wet bulb temperature (scaled)	-0.625	0.226
Relative humidity (scaled)	0.243	0.098
α, density dependence slope (degrees)	56.29	2.37
d, density dependence start	0.58	0.055

Moran curve model. Parameter from Equation 3.		**Standard errors**
λ_0, field fertility (unlimited growth)	1.04	1.02

451

452 ## Alternative model

453 The significant presence of density dependence was also confirmed using a negative binomial
454 generalized mixed linear model as adapted from (Chaves, Imanishi et al. 2015), to fit the
455 environmental stochastic Ricker model (Equation 16). We obtained a density dependence
456 slope equivalent to 78.35 degrees (p-value <0.001) confirming an overcompensating
457 population, although with an intensity stronger than the one obtained by the Moran Curve
458 approach. The covariates coefficients were identical to the mortalities in the intrinsic growth
459 rate framework, however not statistically significant (p-value > 0.05). Summary statistics of
460 the model are shown in supplementary table ST4.

461 ## Mosquito intrinsic growth rate and abundance

462 The intrinsic growth rate is spatially heterogeneous with minimum value of 0, and maximum
463 of 3.66 (a 38 fold increase, as obtained by exponentiating 3.66). The average intrinsic growth
464 rate for the 12 months period was 0.34, a value showing a slight increase in the population
465 (zero is equivalent to birth rate = death rate)(Trajer, Tanczos et al. 2017, Chaves and Moji
466 2018).

467 Mosquito abundance ZIP regression spatio-temporal kriging model parameters are
468 summarised in Table 2. Mosquito abundance is characterised by a shorter spatial range and
469 longer temporal range than mosquito intrinsic growth rate, which describes a larger spatial

heterogeneity and temporal homogeneity than the intrinsic growth rate. The covariate effect's is similar to the one found in the intrinsic growth rate framework (compare coefficients in Table 1 and Table 2).

Table 2. Mosquito abundance modelling. Spatio-temporal Kriging and Moran curve parameters for the residuals obtained from the ZIP model described in Equation 11 and 12. *Standardised so that the sum of the nugget and partial sill is equal to 1.

Parameters	**Value**	
Kriging model: Spatio-temporal covariance		**Envelopes**
ω, spatial range (m)	64.000	13,150
ρ, temporal range (months)	11.000	7,12
Spatial nugget*	0.000	0,0.1
Spatial partial sill*	1.000	0.9,1
Temporal nugget*	0.314	0,0.45
Temporal partial sill*	0.686	0.55,1
ZIP, count part		**Standard errors**
Intercept	-173.521	5.048
Air temperature (scaled)	1.213	0.424
Relative humidity (scaled)	0.173	0.062
Wet bulb temperature (scaled)	-0.907	0.458
Atmospheric pressure	0.158	0.061

Intrinsic growth rate and dengue cases, quantifying the geographic association

The compared models: (i) with no predictors; (ii) mosquito abundance as predictor; (iii) intrinsic growth rate as predictor; (iv) intrinsic growth rate and density of mosquitoes as

predictors; all containing a spatio-temporal Gaussian process and an intercept term, were compared using two information criteria, WAIC and DIC, as described in methods (Gelman, Hwang et al. 2014). Table 3 shows the summary statistics for the four models.

Table 3. Summary statistics for the spatio-temporal log-Cox Gaussian process used to model the dengue cases. In parenthesis the 95% credible interval are reported for each parameter.

Parameter	**Model 1: Intercept only**	**Model 2: Intercept and Abundance**	**Model 3: Intercept and IGR**	**Model 4: Intercept, Abundance and IGR**
$\beta_{\text{intercept}}$	$1.6\ 10^{-8}$ ($1\ 10^{-8}$, $2.2\ 10^{-8}$)	$1.8\ 10^{-8}$ ($9\ 10^{-9}$, $3.1\ 10^{-8}$)	$1.6\ 10^{-8}$ ($1\ 10^{-8}$, $2.6\ 10^{-8}$)	$1.8\ 10^{-8}$ ($9\ 10^{-9}$, $3\ 10^{-8}$)
$\beta_{\text{Abundance}}$	-	0.84 (0.18,1.9)	-	0.99 (0.09,3.9)
β_{IGR}	-	-	0.91 (0.33,1.8)	1.30 (0.25,3.9)
γ	1.9 (1.3,2.5)	1.9 (1.4,2.5)	1.9 (1.4,2.5)	1.9 (1.4,2.6)
ω	138 (78,215)	136 (82,210)	135 (78,209)	136 (79,214)
ρ	8.1 (4.5,20)	7.9 (4.5,19)	7.8 (4.5,18)	7.6 (4.5,16)
WAIC	504.43	505.34	503.88	508.12
DIC	1018.33	1013.58	976.10	958.24

A smaller WAIC and DIC indicates better model predictive accuracy. In both WAIC and DIC model 3 (IGR) outperforms model 2 (abundance). Smaller differences are found between model 1 (intercept only) and model 2. The two information criteria disagree on model 4, ranked as the worst by WAIC and as the best by DIC. However, due to the structure of the model and the approximation to cross-validation of the WAIC penalty term, the WAIC must

493 be considered a more reliable measure compared to DIC. The results therefore show that the
494 order of preference for the models 3, which contains the intercept and IGR, followed by
495 intercept only (model 1). Model 2 composed by intercept and mosquito abundance, and
496 model 3 composed by intercept, mosquito abundance and IGR, do not outperform the null
497 model (model 1). In Figure 4 are shown the averaged predicted number of dengue cases and
498 exceedances for the Caratinga area. The risk is geographically limited around the cases.

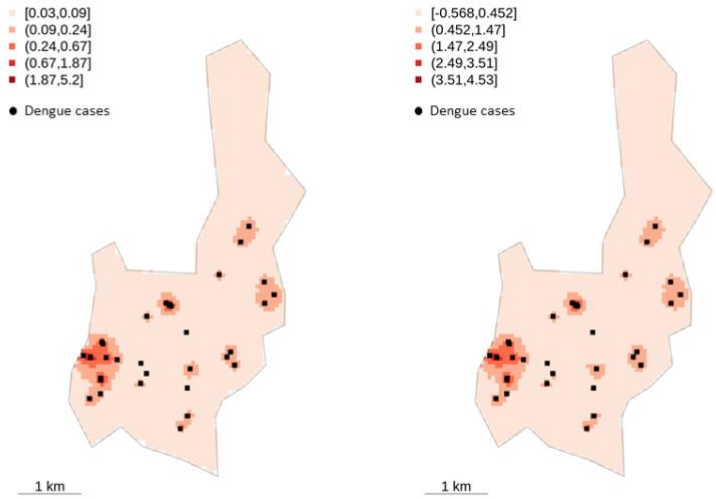

499

500 Figure 4. Weighted average of predicted dengue cases x 1000 people during the 2011/12
501 surveillance campaign (left). On the right is shown the equivalent exceedance map, with exceedance
502 threshold of 0.33 x 1000 people.

503

504 ## Discussion

505 This study shows that the geographic and temporal association of dengue incidence and
506 mosquito intrinsic growth rate is more robust than with mosquito abundance. The latter was
507 found to have a lower predictive accuracy than the former (in terms of WAIC and DIC) and

with small differences compared to the null model. The WAIC and DIC are discordant for the model with both variables (abundance + growth) which may indicate a better inference in model 4 than model 3 but with a lower predictive accuracy (Gelman, Hwang et al. 2014). It also shows that dengue incidence presents a strong spatio-temporal dependence as inferred by the statistically significant parameters employed in the spatio-temporal Gaussian process of the log-Cox model.

It is important to note that this analysis was based on actual dengue cases, i.e. people tested after onset of symptoms, and therefore ignores the characteristics and patterns of dengue infections (ascertained from a serosurveillance campaign (Li, Xu et al. 2019)). A great proportion of infections are likely to be asymptomatic (Slavov, Ciliao-Alves et al. 2019) and the incidence of dengue cases doesn't necessarily correlate with the underlying transmission intensity (Perkins, Reiner et al. 2014). We cannot unrealistically assume that all the infections originated at household location/proximity without considering other important variables that may play a role in the geographic ranges of dengue transmission, such as house quality and socio-economic conditions (Farinelli, Baquero et al. 2018, Lippi, Stewart-Ibarra et al. 2018) or human behaviour and mobility (shopping, schooling etc..)(Stoddard, Forshey et al. 2013, Chuang, Ng et al. 2018, Kraemer, Bisanzio et al. 2018, Sanna, Wu et al. 2018, Wen, Hsu et al. 2018). Road network density may also be an important factor (Li, Cao et al. 2018) and additional analyses are necessary to confirm the spatial pattern found in this work.

Our results are not surprising in the light of conventional disease transmission indices. In fact, the positive association of incidence of dengue cases with the intrinsic growth rate has a similar interpretation as for vectorial capacity and the reproductive number R0. These measures also contain some of the parameters used to calculate intrinsic growth rate (vector mortality), but do not usually account for the additional parameters such as unlimited growth and density dependent and independent mortality. The main advantage in mapping the

intrinsic growth rate with the method presented here, when mosquito surveillance data is available, is that it does not require assumptions of mortality or other population parameters (Desenclos 2011).

Our results suggest (also by using the alternative model comparison) that there may be density dependent mortality for adult *Ae. aegypti* and this has important implications for *Aedes* control (Hancock, White et al. 2016). However, only a year of surveillance may not have differentiated density dependence from seasonal or larger periodic environmental determinants (Vincenti-Gonzalez, Tami et al. 2018). As can be expected from trapping gravid mosquito females, the unlimited growth of 1.04 is well below the theoretical log fertility rate for mosquito (between 4 and 5, when considering 100-200 eggs every 2-3 weeks)(Clemons, Mori et al. 2010, Robert, Legros et al. 2012, Robert, Okamoto et al. 2014). Finally, our results have shown the presence of a mixture of trap populations of different size (supplementary table ST3). Discrepancies between the general (or global) model and results from individual traps may raise concerns about local heterogeneities and therefore the validity of the general model when applied to all the traps locations. This concern may be strengthened by the evidence that local and independent populations are acting in the area, however this does not seem the case for two reasons: (i) previous analyses on the area estimated large scale (for the size of the area) mosquito mobility (Sedda, Vilela et al. 2018) which may be at the origin of a metapopulation for the area of Caratinga; (ii) the overall population has a balanced average growth rate which is at the base of the definition of population (see for example (Berryman 1999) page 14). In practice, assuming a single mosquito population or metapopulation in the area of Caratinga, means modelling the population under maximum limiting factors (see again (Berryman 1999) fifth principle of population dynamics 'limiting factors') which is plausible for a relatively small area (12 km^2).

Not surprisingly temperature and humidity are significantly associated with mosquito adult's mortality. Temperature affects the growth, development and survival of mosquitoes (Attaway, Waters et al. 2017) and is recognised as the most influential predictor of *Aedes* abundance (Weetman, Kamgang et al. 2018), as for most ectotherms, warmer temperatures reduces the size but increases the development rate of *Ae. aegypti* in the aquatic stages (Padmanabha, Correa et al. 2012) (within certain limits (Wang, Tang et al. 2016, Whiten and Peterson 2016)). Wet bulb temperature is a measure based on both temperature and humidity. No previous studies analysed the relationship between wet bulb temperature and *Ae. aegypti* apart from using it as limiting factor (Derrick and Bicks 1958). The negative association may be related to the effect of lower temperature at lower humidity levels. For the latter, the variable relative humidity has been found to increase mortality, again a common association within certain limits (Ferreira, Degener et al. 2017, Lega, Brown et al. 2017). The importance of the atmospheric pressure in the zero-inflated model employed for mosquito abundance is related to the increase in mortality of *Ae. aegypti* at lower atmospheric pressure (Galun and Fraenkel 1961). The significance of these covariates in our frameworks confirms their importance for *Ae. aegypti* and dengue modelling (Li, Xu et al. 2019).

This analysis is based on mapping the intrinsic growth rate observed for female *Aedes* mosquitoes. Recent research shows the adequacy and sometimes the superiority of female mosquito-based indices instead of egg and larvae-based measures to predict dengue risk (Parra, Favaro et al. 2018). Certainly the spatial and temporal ranges found in this work need to be considered carefully before any generalizations (unless as prior-information for future Bayesian framework). These values are related to unexplained environmental conditions, which may change over time. Despite this limitation, the intrinsic growth rate can be used for the accurate estimation of mosquito sources or reservoir areas, which are a priority for the

deployment of mosquito control measures and precision public health (Álvaro Eduardo Eiras 2009, Pepin, Marques-Toledo et al. 2013, Dowell, Blazes et al. 2016).

It is important to note that this work has some limitations. As stated above, we only used 12 months of data which may be not long enough to have full discrimination of density dependence mortality (Hoshi, Higa et al. 2014). Sampling protocols did not detect all individuals at a site, and detection rates may vary among sites, confounding abundance estimates. In addition, this work only considered few climatic variables as environmental forces on mortality. However, food limitation and/or resource competition are major determinants of the rate of *Ae. aegypti* production (Alto, Muturi et al. 2012, Riley, Eames et al. 2015, Wen, Lin et al. 2015, Ruiz-Moreno 2016).

Finally, the dengue outbreak was somewhat limited in size (only 44 dengue cases were analysed), and therefore the results of the spatio-temporal Gaussian log-cox model must be treated with caution. In addition, we cannot exclude that other mosquito abundance-based metrics (ratio of abundance between two periods of time or abundance greater than a given threshold) may perform better than intrinsic growth rate. This work concentrates on the simple comparison between intrinsic growth rate and abundance which are the most common describer used for population dynamics and population distribution/suitability respectively.

Conclusions

Achieving the global dengue control strategy (the major and most diffuse disease spread by *Aedes*), which calls for at least 50% reduction in the disease mortality burden and a minimum of 25% reduction in incidence by 2020 (World Health Organization 2012), requires innovative approaches and interventions that go beyond simple disease surveillance or ecological analyses. In this paper, we propose a biological-statistical framework that may

serve for vector control spatial targeting. Our aim is to improve current vector surveillance programmes that are lacking in effective measurement of certain vector indicators, and we hope to promote a debate among biologist, mathematicians/statisticians and field workers about the optimal vector indices required for vector-borne disease elimination and eradication. Many of the mosquito-borne diseases do not have effective vaccines or treatments and are controlled by mosquito elimination (Robert, Okamoto et al. 2014, Evans, Gloria-Soria et al. 2015), or by preventing vector contact (Reyes-Solis, Saavedra-Rodriguez et al. 2014). The same framework can support successful interventions by identifying mosquito sources. For example, this could be applied to field trials with *Wolbachia* infected mosquitoes to reduce dengue transmission (Caragata, Dutra et al. 2016, Achee, Grieco et al. 2019). The present results require large scale investigations to confirm the significance of our study. The implications are obvious in terms of disease control, but also for disease surveillance and forecasting (Schwab, Stone et al. 2018), especially for a disease like dengue that has a high probability of spatial recurrence in urban areas (Chen, Ong et al. 2018).

Competing interests

The authors declare that they have no competing interests.

References

Achee, N. L., J. P. Grieco, H. Vatandoost, G. Seixas, J. Pinto, L. Ching-Ng, A. J. Martins, W. Juntarajumnong, V. Corbel, C. Gouagna, J. P. David, J. G. Logan, J. Orsborne, E. Marois, G. J. Devine and J. Vontas (2019). "Alternative strategies for mosquito-borne arbovirus control." PLoS Negl Trop Dis **13**(1): e0006822.

Allen, J. C., C. C. Brewster and D. H. Slone (2001). "Spatially explicit ecological models: a spatial convolution approach." Chaos Solitons & Fractals **12**(2): 333-347.

Alto, B. W., E. J. Muturi and R. L. Lampman (2012). "Effects of nutrition and density in Culex pipiens." Medical and Veterinary Entomology **26**(4): 396-406.

Álvaro Eduardo Eiras, M. C. R. (2009). "Preliminary evaluation of the “Dengue-MI” technology for Aedes aegypti monitoring and control." Caderno de Saúde Pública Rio de Janeiro **25**(1): 14.

Armbruster, P. A. (2016). "Photoperiodic Diapause and the Establishment of Aedes albopictus (Diptera: Culicidae) in North America." Journal of Medical Entomology **53**(5): 1013-1023.

Attaway, D. F., N. M. Waters, E. M. Geraghty and K. H. Jacobsen (2017). "Zika virus: Endemic and epidemic ranges of Aedes mosquito transmission." Journal of Infection and Public Health **10**(1): 120-123.
Berryman, A. A. (1999). Principles of Population Dynamics and Their Application, Stanley Thornes.
Bowman, L. R., S. Donegan and P. J. McCall (2016). "Is Dengue Vector Control Deficient in Effectiveness or Evidence?: Systematic Review and Meta-analysis." Plos Neglected Tropical Diseases **10**(3).
Brady, O. J., N. Golding, D. M. Pigott, M. U. G. Kraemer, J. P. Messina, R. C. Reiner, T. W. Scott, D. L. Smith, P. W. Gething and S. I. Hay (2014). "Global temperature constraints on Aedes aegypti and Ae. albopictus persistence and competence for dengue virus transmission." Parasites & Vectors **7**.
Caragata, E. P., H. L. C. Dutra and L. A. Moreira (2016). "Exploiting Intimate Relationships: Controlling Mosquito-Transmitted Disease with Wolbachia." Trends Parasitol **32**(3): 207-218.
Chambers, J. (2008). Software for Data Analysis: Programming with R, Springer New York.
Chaves, L. F., N. Imanishi and T. Hoshi (2015). "Population dynamics of Armigeres subalbatus (Diptera: Culicidae) across a temperate altitudinal gradient." Bulletin of Entomological Research **105**(5): 589-597.
Chaves, L. F. and K. Moji (2018). "Density Dependence, Landscape, and Weather Impacts on Aquatic Aedes japonicus japonicus (Diptera: Culicidae) Abundance Along an Urban Altitudinal Gradient." Journal of Medical Entomology **55**(2): 329-341.
Chen, Y. R., J. H. Y. Ong, J. Rajarethinam, G. Yap, L. C. Ng and A. R. Cook (2018). "Neighbourhood level real-time forecasting of dengue cases in tropical urban Singapore." Bmc Medicine **16**.
Chuang, T. W., K. C. Ng, T. L. Nguyen and L. F. Chaves (2018). "Epidemiological Characteristics and Space-Time Analysis of the 2015 Dengue Outbreak in the Metropolitan Region of Tainan City, Taiwan." International Journal of Environmental Research and Public Health **15**(3).
Cianci, D., N. Hartemink, C. B. Zeimes, S. O. Vanwambeke, A. Ienco and B. Caputo (2015). "High resolution spatial analysis of habitat preference of Aedes albopictus (diptera: Culicidae) in an urban environment." Journal of Medical Entomology **52**(3): 329-335.
Clemons, A., A. Mori, M. Haugen, D. W. Severson and M. Duman-Scheel (2010). "Culturing and egg collection of Aedes aegypti." Cold Spring Harb Protoc **2010**(10): pdb prot5507.
Consoli, R. A. G. B. and R. L. o. d. Oliveira (1994). Principais mosquitos de importância sanitária no Brasil. Rio de Janeiro, RJ, Editora FIOCRUZ.
Cortes, F., C. M. Turchi Martelli, R. Arraes de Alencar Ximenes, U. R. Montarroyos, J. B. Siqueira Junior, O. Goncalves Cruz, N. Alexander and W. Vieira de Souza (2018). "Time series analysis of dengue surveillance data in two Brazilian cities." Acta Trop **182**: 190-197.
Cromwell, E. A., S. T. Stoddard, C. M. Barker, A. Van Rie, W. B. Messer, S. R. Meshnick, A. C. Morrison and T. W. Scott (2017). "The relationship between entomological indicators of Aedes aegypti abundance and dengue virus infection." Plos Neglected Tropical Diseases **11**(3).
de Thoisy, B., V. Lacoste, A. Germain, J. Munoz-Jordan, C. Colon, J. F. Mauffrey, M. Delaval, F. Catzeflis, M. Kazanji, S. Matheus, P. Dussart, J. Morvan, A. A. Setien, X. Deparis and A. Lavergne (2009). "Dengue infection in neotropical forest mammals." Vector Borne Zoonotic Dis **9**(2): 157-170.
Derrick, E. H. and V. A. Bicks (1958). "The limiting temperature for the transmission of dengue." Australasian Annals of Medicine **7**(2): 102-107.
Desenclos, J. C. (2011). "Transmission parameters of vector-borne infections." Medecine Et Maladies Infectieuses **41**(11): 588-593.
Diallo, M., Y. Ba, A. A. Sall, O. M. Diop, J. A. Ndione, M. Mondo, L. Girault and C. Mathiot (2003). "Amplification of the sylvatic cycle of dengue virus type 2, Senegal, 1999-2000: entomologic findings and epidemiologic considerations." Emerg Infect Dis **9**(3): 362-367.
Dowell, S. F., D. Blazes and S. Desmond-Hellmann (2016). "Four steps to precision public health." Nature **540**(7632): 189-191.
Ehrlen, J. and W. F. Morris (2015). "Predicting changes in the distribution and abundance of species under environmental change." Ecology Letters **18**(3): 303-314.

687 Elderd, B. (2017). Modeling Insect Epizootics and their Population-Level Consequences. Ecology of
688 Invertebrate Diseases**:** 441-467.
689 Evans, B. R., A. Gloria-Soria, L. Hou, C. McBride, M. Bonizzoni, H. Zhao and J. R. Powell (2015). "A
690 multipurpose, high-throughput single-nucleotide polymorphism chip for the dengue and yellow
691 fever mosquito, Aedes aegypti." G3: Genes, Genomes, Genetics **5**(5): 711-718.
692 Fares, R. C., K. P. Souza, G. Anez and M. Rios (2015). "Epidemiological Scenario of Dengue in Brazil."
693 Biomed Res Int **2015**: 321873.
694 Farinelli, E. C., O. S. Baquero, C. Stephan and F. Chiaravalloti-Neto (2018). "Low socioeconomic
695 condition and the risk of dengue fever: A direct relationship." Acta Tropica **180**: 47-57.
696 Favaro, E. A., M. R. Dibo, A. Mondini, A. C. Ferreira, A. A. C. Barbosa, A. E. Eiras, E. A. M. F. Barata and
697 F. Chiaravalloti-Neto (2006). "Physiological state of Aedes (Stegomyia) aegypti mosquitoes captured
698 with MosquiTRAPs (TM) in Mirassol, Sao Paulo, Brazil." Journal of Vector Ecology **31**(2): 285-291.
699 Ferreira, D. A. D., C. M. Degener, C. D. Marques-Toledo, M. M. Bendati, L. O. Fetzer, C. P. Teixeira
700 and A. E. Eiras (2017). "Meteorological variables and mosquito monitoring are good predictors for
701 infestation trends of Aedes aegypti, the vector of dengue, chikungunya and Zika." Parasites &
702 Vectors **10**.
703 Galun, R. and G. Fraenkel (1961). "The effect of low atmospheric pressure on adult Aedes aegypti
704 and on housefly pupae." Journal of Insect Physiology **7**(3): 161-176.
705 Gelman, A., J. Hwang and A. Vehtari (2014). "Understanding predictive information criteria for
706 Bayesian models." Statistics and Computing **24**(6): 997-1016.
707 Gerber, L. R., H. McCallum, K. D. Lafferty, J. L. Sabo and A. Dobson (2005). "Exposing extinction risk
708 analysis to pathogens: Is disease just another form of density dependence?" Ecological Applications
709 **15**(4): 1402-1414.
710 Hancock, P. A., V. L. White, S. A. Ritchie, A. A. Hoffmann and H. C. J. Godfray (2016). "Predicting
711 Wolbachia invasion dynamics in Aedes aegypti populations using models of density-dependent
712 demographic traits." BMC Biology **14**(1).
713 Hassell, M. P., H. N. Comins and R. M. May (1991). "Spatial Structure and Chaos in Insect Population-
714 Dynamics." Nature **353**(6341): 255-258.
715 Hastie, T. J. (2017). Statistical Models in S, CRC Press.
716 Herrando-Pérez, S., S. Delean, B. W. Brook and C. J. A. Bradshaw (2012). "Density dependence: An
717 ecological Tower of Babel." Oecologia **170**(3): 585-603.
718 Hoshi, T., Y. Higa and L. F. Chaves (2014). "Uranotaenia novobscura ryukyuana (Diptera: Culicidae)
719 population dynamics are denso-dependent and autonomous from weather fluctuations." Annals of
720 the Entomological Society of America **107**(1): 136-142.
721 Hoshi, T., N. Imanishi, K. Moji and L. F. Chaves (2017). "Density dependence in a seasonal time series
722 of the bamboo mosquito, Tripteroides bambusa (Diptera: Culicidae)." Canadian Entomologist **149**(3):
723 338-344.
724 Jian, Y., S. Silvestri, E. Belluco, A. Saltarin, G. Chillemi and M. Marani (2014). "Environmental forcing
725 and density-dependent controls of Culex pipiens abundance in a temperate climate (Northeastern
726 Italy)." Ecological Modelling **272**: 301-310.
727 Jian, Y., S. Silvestri, J. Brown, R. Hickman and M. Marani (2014). "The temporal spectrum of adult
728 mosquito population fluctuations: Conceptual and modeling implications." PLoS ONE **9**(12).
729 Kraemer, M. U., M. E. Sinka, K. A. Duda, A. Mylne, F. M. Shearer, O. J. Brady, J. P. Messina, C. M.
730 Barker, C. G. Moore, R. G. Carvalho, G. E. Coelho, W. Van Bortel, G. Hendrickx, F. Schaffner, G. R.
731 Wint, I. R. Elyazar, H. J. Teng and S. I. Hay (2015). "The global compendium of Aedes aegypti and Ae.
732 albopictus occurrence." Sci Data **2**: 150035.
733 Kraemer, M. U. G., D. Bisanzio, R. C. Reiner, R. Zakar, J. B. Hawkins, C. C. Freifeld, D. L. Smith, S. I.
734 Hay, J. S. Brownstein and T. A. Perkins (2018). "Inferences about spatiotemporal variation in dengue
735 virus transmission are sensitive to assumptions about human mobility: a case study using geolocated
736 tweets from Lahore, Pakistan." Epj Data Science **7**.

Lambert, D. (1992). "Zero-Inflated Poisson Regression, with an Application to Defects in Manufacturing." Technometrics **34**(1): 1-14.
Lana, R. M., T. G. S. Carneiro, N. A. Honório and C. T. Codeço (2014). "Seasonal and nonseasonal dynamics of Aedes aegypti in Rio de Janeiro, Brazil: Fitting mathematical models to trap data." Acta Tropica **129**(1): 25-32.
Lega, J., H. E. Brown and R. Barrera (2017). "Aedes aegypti (Diptera: Culicidae) Abundance Model Improved With Relative Humidity and Precipitation-Driven Egg Hatching." Journal of Medical Entomology **54**(5): 1375-1384.
Legros, M., M. Otero, V. R. Aznar, H. Solari, F. Gould and A. L. Lloyd (2016). "Comparison of two detailed models of Aedes aegypti population dynamics." Ecosphere **7**(10).
Li, Q. X., W. Cao, H. Y. Ren, Z. L. Ji and H. X. Jiang (2018). "Spatiotemporal responses of dengue fever transmission to the road network in an urban area." Acta Tropica **183**: 8-13.
Li, R., L. Xu, O. N. Bjørnstad, K. Liu, T. Song, A. Chen, B. Xu, Q. Liu and N. C. Stenseth (2019). "Climate-driven variation in mosquito density predicts the spatiotemporal dynamics of dengue." Proceedings of the National Academy of Sciences **116**(9): 3624-3629.
Lippi, C. A., A. M. Stewart-Ibarra, A. G. Munoz, M. J. Borbor-Cordova, R. Mejia, K. Rivero, K. Castillo, W. B. Cardenas and S. J. Ryan (2018). "The Social and Spatial Ecology of Dengue Presence and Burden during an Outbreak in Guayaquil, Ecuador, 2012." International Journal of Environmental Research and Public Health **15**(4).
Ministério da Agricultura, P. e. A. (2015). "Instituto Nacional de Metereologia." Retrieved 10/01/2015, 2015, from http://www.inmet.gov.br/portal.
Padmanabha, H., F. Correa, M. Legros, H. F. Nijhout, C. Lord and L. P. Lounibos (2012). "An eco-physiological model of the impact of temperature on Aedes aegypti life history traits." Journal of Insect Physiology **58**(12): 1597-1608.
Parham, P. E., D. Pople, C. Christiansen-Jucht, S. Lindsay, W. Hinsley and E. Michael (2012). "Modeling the role of environmental variables on the population dynamics of the malaria vector Anopheles gambiae sensu stricto." Malaria Journal **11**.
Parra, M. C. P., E. A. Favaro, M. R. Dibo, A. Mondini, A. E. Eiras, E. G. Kroon, M. M. Teixeira, M. L. Nogueira and F. Chiaravalloti-Neto (2018). "Using adult & IT;Aedes aegypti & IT; females to predict areas at risk for dengue transmission: A spatial case-control study." Acta Tropica **182**: 43-53.
Pepin, K. M., C. Marques-Toledo, L. Scherer, M. M. Morais, B. Ellis and A. E. Eiras (2013). "Cost-effectiveness of novel system of mosquito surveillance and control, Brazil." Emerg Infect Dis **19**(4): 542-550.
Perkins, T. A., R. C. Reiner, I. Rodriguez-Barraquer, D. L. Smith, T. W. Scott and D. A. Cummings (2014). "A review of transmission models of dengue: a quantitative and qualitative analysis of model features." Dengue and dengue hemorrhagic fever. 2nd ed. Wallingford: CABI: 99-114.
Phuc, H. K., M. H. Andreasen, R. S. Burton, C. Vass, M. J. Epton, G. Pape, G. Fu, K. C. Condon, S. Scaife, C. A. Donnelly, P. G. Coleman, H. White-Cooper and L. Alphey (2007). "Late-acting dominant lethal genetic systems and mosquito control." BMC Biol **5**: 11.
Reiner, R. C., T. A. Perkins, C. M. Barker, T. Niu, L. F. Chaves, A. M. Ellis, D. B. George, A. Le Menach, J. R. Pulliam and D. Bisanzio (2013). "A systematic review of mathematical models of mosquito-borne pathogen transmission: 1970–2010." Journal of The Royal Society Interface **10**(81): 20120921.
Reyes-Solis, G. e., K. Saavedra-Rodriguez, A. F. Suarez and W. C. Black (2014). "QTL mapping of genome regions controlling temephos resistance in larvae of the mosquito Aedes aegypti." PLoS neglected tropical diseases **8**(10): e3177.
Riley, S., K. Eames, V. Isham, D. Mollison and P. Trapman (2015). "Five challenges for spatial epidemic models." Epidemics **10**: 68-71.
Robert, M. A., M. Legros, L. Facchinelli, L. Valerio, J. M. Ramsey, T. W. Scott, F. Gould and A. L. Lloyd (2012). "Mathematical models as aids for design and development of experiments: The case of transgenic mosquitoes." Journal of Medical Entomology **49**(6): 1177-1188.

787 Robert, M. A., K. W. Okamoto, F. Gould and A. L. Lloyd (2014). "Antipathogen genes and the
788 replacement of disease-vectoring mosquito populations: A model-based evaluation." Evolutionary
789 Applications **7**(10): 1238-1251.
790 Rodriguez-Barraquer, I., M. T. Cordeiro, C. Braga, W. V. de Souza, E. T. Marques and D. A. T.
791 Cummings (2011). "From Re-Emergence to Hyperendemicity: The Natural History of the Dengue
792 Epidemic in Brazil." Plos Neglected Tropical Diseases **5**(1).
793 Rogers, D. (1979). "Tsetse Population-Dynamics and Distribution - New Analytical Approach." Journal
794 of Animal Ecology **48**(3): 825-849.
795 Royle, J. A. (2004). "N-mixture models for estimating population size from spatially replicated
796 counts." Biometrics **60**(1): 108-115.
797 Ruiz-Moreno, D. (2016). "Assessing Chikungunya risk in a metropolitan area of Argentina through
798 satellite images and mathematical models." BMC Infectious Diseases **16**(1).
799 Sanna, M., J. Y. Wu, Y. S. Zhu, Z. C. Yang, J. H. Lu and Y. H. Hsieh (2018). "Spatial and Temporal
800 Characteristics of 2014 Dengue Outbreak in Guangdong, China." Scientific Reports **8**.
801 Sarfraz, M. S., N. K. Tripathi, F. S. Faruque, U. I. Bajwa, A. Kitamoto and M. Souris (2014). "Mapping
802 urban and peri-urban breeding habitats of Aedes mosquitoes using a fuzzy analytical hierarchical
803 process based on climatic and physical parameters." Geospatial Health **8**(3): S685-S697.
804 Sarfraz, M. S., N. K. Tripathi, T. Tipdecho, T. Thongbu, P. Kerdthong and M. Souris (2012). "Analyzing
805 the spatio-temporal relationship between dengue vector larval density and land-use using factor
806 analysis and spatial ring mapping." BMC Public Health **12**(1).
807 Saúde, M. d. (2015). "DATASUS - Sinan." Retrieved 12/01/2015, from
808 http://tabnet.datasus.gov.br/cgi/deftohtm.exe?sinannet/dengue/bases/denguebrnet.def.
809 Schaffner, F., R. Bellini, D. Petrić, E. J. Scholte, H. Zeller and L. Marrama Rakotoarivony (2013).
810 "Development of guidelines for the surveillance of invasive mosquitoes in Europe." Parasites and
811 Vectors **6**(1).
812 Schwab, S. R., C. M. Stone, D. M. Fonseca and N. H. Fefferman (2018). "The importance of being
813 urgent: The impact of surveillance target and scale on mosquito-borne disease control." Epidemics
814 **23**: 55-63.
815 Sedda, L., C. Mweempwa, E. Ducheyne, C. De Pus, G. Hendrickx and D. J. Rogers (2014). "A Bayesian
816 Geostatistical Moran Curve Model for Estimating Net Changes of Tsetse Populations in Zambia." Plos
817 One **9**(4).
818 Sedda, L., A. P. P. Vilela, E. R. G. R. Aguiar, C. H. P. Gaspar, A. N. A. Goncalves, R. P. Olmo, A. T. S.
819 Silva, L. D. da Silveira, A. E. Eiras, B. P. Drumond, E. G. Kroon and J. T. Marques (2018). "The spatial
820 and temporal scales of local dengue virus transmission in natural settings: a retrospective analysis."
821 Parasites & Vectors **11**.
822 Slavov, S. N., D. C. Ciliao-Alves, F. A. C. Gonzaga, D. R. Moura, A. de Moura, L. A. G. de Noronha, E. M.
823 Cassemiro, B. M. S. Pimentel, F. J. Q. Costa, G. A. da Silva, D. Ramos, W. N. de Araujo, S. Kashima and
824 R. Haddad (2019). "Dengue seroprevalence among asymptomatic blood donors during an epidemic
825 outbreak in Central-West Brazil." PLoS One **14**(3): e0213793.
826 Stoddard, S. T., B. M. Forshey, A. C. Morrison, V. A. Paz-Soldan, G. M. Vazquez-Prokopec, H. Astete,
827 R. C. Reiner, Jr., S. Vilcarromero, J. P. Elder, E. S. Halsey, T. J. Kochel, U. Kitron and T. W. Scott (2013).
828 "House-to-house human movement drives dengue virus transmission." Proc Natl Acad Sci U S A
829 **110**(3): 994-999.
830 Tatem, A. J. (2017). "Comment: WorldPop, open data for spatial demography." Scientific Data **4**.
831 Taylor, B. M. (2019). lgcpGPU: Inference for aggregated spatiotemporal log-Gaussian Cox processes
832 with changing support via GPU computing. https://gitlab.com/ben_taylor/lgcpGPU.
833 Taylor, B. M., R. Andrade-Pacheco and H. J. W. Sturrock (2018). "Continuous inference for
834 aggregated point process data." Journal of the Royal Statistical Society Series a-Statistics in Society
835 **181**(4): 1125-1150.
836 Tonnang, H. E. Z., B. D. B. Hervé, L. Biber-Freudenberger, D. Salifu, S. Subramanian, V. B. Ngowi, R. Y.
837 A. Guimapi, B. Anani, F. M. M. Kakmeni, H. Affognon, S. Niassy, T. Landmann, F. T. Ndjomatchoua, S.

A. Pedro, T. Johansson, C. M. Tanga, P. Nana, K. M. Fiaboe, S. F. Mohamed, N. K. Maniania, S. Ekesi and C. Borgemeister (2017). "Advances in crop insect modelling methods—Towards a whole system approach." Ecological Modelling **354**: 88-103.
Trajer, A., B. Tanczos, T. Hammer, A. Bede-Fazekas, K. A. Ranvig, J. Schoffhauzer and J. Padisak (2017). "The Complex Investigation of the Colonization Potential of Aedes Albopictus (Diptera: Culicidae) in the South Pannonian Ecoregion." Applied Ecology and Environmental Research **15**(1): 275-298.
Turchin, P. (2003). Complex Population Dynamics: A Theoretical/empirical Synthesis, Princeton University Press.
Vargas, W. P., H. Kawa, P. C. Sabroza, V. B. Soares, N. A. Honorio and A. S. de Almeida (2015). "Association among house infestation index, dengue incidence, and sociodemographic indicators: surveillance using geographic information system." Bmc Public Health **15**.
Varley, G. C. and G. R. Gradwell (1960). "Key Factors in Population Studies." Journal of Animal Ecology **29**(2): 399-401.
Varley, G. C., G. R. Gradwell and M. P. Hassell (1973). Insect Population Ecology: An Analytical Approach, Blackwell Scientific.
Vehtari, A., A. Gelman and J. Gabry (2016). "Practical Bayesian model evaluation using leave-one-out cross-validation and WAIC." Statistics and Computing **27**(5): 1413-1432.
Vincenti-Gonzalez, M. F., A. Tami, E. F. Lizarazo and M. E. Grillet (2018). "ENSO-driven climate variability promotes periodic major outbreaks of dengue in Venezuela." Sci Rep **8**(1): 5727.
Walker, D. D., J. C. Loftis and P. W. Mielke (1997). "Permutation methods for determining the significance of spatial dependence." Mathematical Geology **29**(8): 1011-1024.
Wang, X., S. Y. Tang and R. A. Cheke (2016). "A stage structured mosquito model incorporating effects of precipitation and daily temperature fluctuations." Journal of Theoretical Biology **411**: 27-36.
Weetman, D., B. Kamgang, A. Badolo, C. L. Moyes, F. M. Shearer, M. Coulibaly, J. Pinto, L. Lambrechts and P. J. McCall (2018). "Aedes Mosquitoes and Aedes-Borne Arboviruses in Africa: Current and Future Threats." International journal of environmental research and public health **15**(2): 220.
Wen, T. H., C. S. Hsu and M. C. Hu (2018). "Evaluating neighborhood structures for modeling intercity diffusion of large-scale dengue epidemics." International Journal of Health Geographics **17**.
Wen, T. H., M. H. Lin, H. J. Teng and N. T. Chang (2015). "Incorporating the human-Aedes mosquito interactions into measuring the spatial risk of urban dengue fever." Applied Geography **62**: 256-266.
Whiten, S. R. and R. K. D. Peterson (2016). "The Influence of Ambient Temperature on the Susceptibility of Aedes aegypti (Diptera: Culicidae) to the Pyrethroid Insecticide Permethrin." Journal of Medical Entomology **53**(1): 139-143.
World Health Organization (2009). Dengue: guidelines for diagnosis, treatment, prevention and control, World Health Organization.
World Health Organization (2012). "Global strategy for dengue prevention and control, 2012-2020." WHO Library Cataloguing-in-Publication Data, Switzerland.
World Health Organization (2014). "A global brief on vector-borne diseases."
Zeileis, A., C. Kleiber and S. Jackman (2008). "Regression models for count data in R." Journal of Statistical Software **27**(8): 1-25.

Supplementary Tables

Supplementary table ST1. Number of caught Ae. aegypti per trap and per month and relative statistics.

Trap ID	Jan	Feb	Mar	Apr	May	Jun	Jul	Aug	Sep	Oct	Nov	Dec	Min	Mean	Max
3	0	1	0	0	0	0	0	0	0	0	0	0	0	0.08	1
4	0	0	0	2	0	0	0	0	0	0	0	0	0	0.17	2
5	0	0	2	0	0	0	0	0	1	1	1	0	0	0.42	2
6	0	0	2	0	0	0	0	0	0	0	0	0	0	0.17	2
8	0	6	6	0	2	0	0	0	1	1	0	6	0	1.83	6
10	0	0	0	0	0	0	0	0	1	0	0	0	0	0.08	1
13	0	0	0	0	0	1	0	0	0	0	0	0	0	0.08	1
14	0	0	0	1	0	0	0	0	0	0	0	0	0	0.08	1
15	0	1	0	1	0	0	0	0	0	0	0	0	0	0.17	1
17	0	0	0	0	0	0	0	1	0	0	0	0	0	0.08	1
19	0	1	1	5	1	0	0	0	0	0	0	1	0	0.75	5
20	0	0	0	1	0	0	0	1	0	1	0	0	0	0.25	1
21	0	0	0	0	1	0	0	0	0	0	0	0	0	0.08	1
22	0	0	0	0	1	0	0	0	0	0	0	0	0	0.08	1
23	0	2	1	0	0	0	0	0	0	0	0	1	0	0.33	2
24	1	0	3	0	1	2	0	1	0	0	0	1	0	0.75	3
25	0	3	0	1	0	0	0	1	0	0	0	1	0	0.50	3
26	0	0	0	1	0	0	0	0	0	0	0	0	0	0.08	1
30	1	3	0	1	0	0	0	0	0	0	0	4	0	0.75	4
32	1	0	0	2	0	0	0	1	0	0	0	0	0	0.33	2
34	0	2	0	0	0	0	0	0	0	0	1	0	0	0.25	2

35	0	0	0	0	1	0	0	1	0	0	0	1	0	0.25	1
36	0	0	2	1	0	1	0	1	0	0	0	1	0	0.50	2
37	0	0	0	0	0	0	0	0	0	0	0	1	0	0.08	1
38	2	0	0	0	0	0	0	0	0	0	0	0	0	0.17	2
39	5	0	0	1	0	0	0	1	0	1	0	0	0	0.67	5
41	0	2	0	0	0	0	0	1	0	0	0	0	0	0.25	2
42	2	0	0	0	0	0	0	0	0	0	0	1	0	0.25	2
45	0	0	0	0	0	1	0	0	0	0	0	0	0	0.08	1
46	1	0	1	7	1	0	0	0	0	0	0	4	0	1.17	7
47	1	0	0	0	0	0	0	0	0	0	0	0	0	0.08	1
49	3	2	3	0	1	0	0	0	1	1	1	3	0	1.25	3
50	1	0	0	1	0	0	0	0	0	0	0	0	0	0.17	1
51	0	0	0	0	0	0	0	1	0	0	0	0	0	0.08	1
52	2	1	0	0	0	1	0	1	0	0	0	7	0	1.00	7
54	4	2	0	0	1	0	0	0	0	1	1	1	0	0.83	4
57	0	0	0	1	1	0	0	0	0	0	0	2	0	0.33	2
58	0	0	0	0	0	0	0	0	0	0	0	1	0	0.08	1
59	0	0	0	0	0	2	0	1	0	0	0	0	0	0.25	2
62	0	0	0	0	1	0	0	0	0	0	0	0	0	0.08	1
64	1	1	0	1	0	0	0	0	1	0	1	1	0	0.50	1
65	5	0	0	0	0	0	0	4	0	1	0	1	0	0.92	5
66	0	3	1	1	0	0	0	0	0	0	0	1	0	0.50	3
67	0	0	1	0	0	1	0	0	0	0	0	0	0	0.17	1
69	0	0	0	0	0	0	0	0	0	0	0	1	0	0.08	1
70	0	3	1	1	1	2	0	1	0	1	0	3	0	1.08	3

71	2	7	0	0	0	0	0	0	0	2	0	1	0	1.00	7
72	2	5	5	1	1	0	0	0	0	0	0	0	0	1.17	5
73	0	0	0	1	1	0	0	0	0	0	0	0	0	0.17	1
74	0	0	0	0	0	1	1	0	0	0	0	2	0	0.33	2
75	0	0	1	0	0	0	0	0	0	0	0	0	0	0.08	1
76	3	1	1	6	1	0	3	0	0	0	0	2	0	1.42	6
77	1	1	1	0	0	0	0	0	0	0	1	0	0	0.33	1
78	0	0	0	5	0	0	0	1	0	0	0	0	0	0.50	5
79	0	0	1	1	0	0	0	0	0	0	0	2	0	0.33	2
80	0	0	1	0	0	0	0	0	0	0	0	0	0	0.08	1
81	3	2	0	2	5	0	0	1	0	0	0	0	0	1.08	5
83	1	5	3	1	1	0	0	0	0	0	0	0	0	0.92	5
85	0	4	0	0	0	0	0	0	0	0	0	3	0	0.58	4
86	0	0	0	0	0	0	0	0	4	0	0	0	0	0.33	4
87	0	1	1	1	0	0	0	0	0	0	0	0	0	0.25	1
90	0	4	1	3	0	1	0	1	0	0	0	8	0	1.50	8
92	0	3	0	6	1	0	1	0	1	0	0	4	0	1.33	6
93	0	0	0	0	1	0	0	0	0	0	0	0	0	0.08	1
95	0	0	0	1	0	0	0	0	0	0	0	0	0	0.08	1
96	0	1	0	0	0	0	1	0	0	0	0	1	0	0.25	1
98	0	0	0	0	0	0	2	0	0	0	0	0	0	0.17	2
100	0	1	0	0	0	0	0	0	0	0	0	0	0	0.08	1
101	0	1	0	0	0	0	0	0	0	0	0	0	0	0.08	1
102	0	0	1	0	0	0	0	0	0	0	0	1	0	0.17	1
103	0	0	1	1	0	1	1	0	1	0	0	0	0	0.42	1

105	1	2	2	5	1	0	0	1	0	0	0	0	0	1.00	5
106	3	1	0	1	0	0	0	0	0	0	0	2	0	0.58	3
107	0	0	0	1	0	0	1	0	1	0	0	1	0	0.33	1
110	0	1	0	0	0	0	0	0	0	0	0	0	0	0.08	1
112	0	0	0	0	0	1	0	0	0	1	0	0	0	0.17	1
113	0	0	1	0	0	0	0	0	0	0	0	0	0	0.08	1
116	1	0	0	1	0	0	0	0	0	0	0	1	0	0.25	1
117	0	0	0	0	0	0	0	0	1	0	0	0	0	0.08	1
118	0	0	0	0	0	0	0	0	0	1	0	0	0	0.08	1
119	0	1	0	0	0	1	0	0	0	0	0	0	0	0.17	1
122	0	2	0	1	0	0	0	0	0	0	0	0	0	0.25	2
123	0	0	1	1	0	0	0	0	1	0	0	2	0	0.42	2
124	0	2	0	3	0	0	1	0	0	0	0	0	0	0.50	3
125	0	0	0	0	0	0	0	0	0	0	1	0	0	0.08	1
126	0	3	1	0	0	0	0	0	0	0	0	0	0	0.33	3
127	0	0	0	0	0	0	0	0	1	0	0	0	0	0.08	1
128	0	1	1	0	1	0	0	0	0	0	0	0	0	0.25	1
129	1	3	8	9	5	4	3	0	1	1	2	1	0	3.17	9
131	1	2	0	3	0	0	0	0	0	2	0	6	0	1.17	6
132	0	0	0	3	0	0	0	0	0	0	0	1	0	0.33	3
133	0	0	0	1	0	0	0	1	0	0	0	0	0	0.17	1
135	3	7	8	2	8	4	0	1	3	1	2	16	0	4.58	16
138	5	2	1	4	0	0	0	0	0	0	3	3	0	1.50	5
139	0	2	0	0	0	0	2	0	0	0	0	0	0	0.33	2
140	0	0	0	0	0	0	2	0	0	0	0	0	0	0.17	2

144	0	2	0	0	0	0	0	0	0	0	0	0	0	0.17	2
147	0	0	0	1	0	0	1	0	3	1	0	0	0	0.50	3
148	0	3	2	0	0	0	1	0	1	0	0	0	0	0.58	3
149	0	0	0	0	0	0	0	0	1	0	0	3	0	0.33	3
150	0	3	2	0	5	0	0	0	0	0	0	0	0	0.83	5
151	0	2	2	0	2	0	1	2	0	0	2	2	0	1.08	2
154	0	0	0	0	0	0	0	0	0	0	1	0	0	0.08	1
160	3	2	4	7	3	1	0	0	1	1	2	5	0	2.42	7
1	0	0	0	0	0	0	0	0	0	0	0	0	0	0.00	0
2	0	0	0	0	0	0	0	0	0	0	0	0	0	0.00	0
7	0	0	0	0	0	0	0	0	0	0	0	0	0	0.00	0
9	0	0	0	0	0	0	0	0	0	0	0	0	0	0.00	0
11	0	0	0	0	0	0	0	0	0	0	0	0	0	0.00	0
12	0	0	0	0	0	0	0	0	0	0	0	0	0	0.00	0
16	0	0	0	0	0	0	0	0	0	0	0	0	0	0.00	0
18	0	0	0	0	0	0	0	0	0	0	0	0	0	0.00	0
27	0	0	0	0	0	0	0	0	0	0	0	0	0	0.00	0
28	0	0	0	0	0	0	0	0	0	0	0	0	0	0.00	0
29	0	0	0	0	0	0	0	0	0	0	0	0	0	0.00	0
31	0	0	0	0	0	0	0	0	0	0	0	0	0	0.00	0
33	0	0	0	0	0	0	0	0	0	0	0	0	0	0.00	0
40	0	0	0	0	0	0	0	0	0	0	0	0	0	0.00	0
43	0	0	0	0	0	0	0	0	0	0	0	0	0	0.00	0
44	0	0	0	0	0	0	0	0	0	0	0	0	0	0.00	0
48	0	0	0	0	0	0	0	0	0	0	0	0	0	0.00	0

53	0	0	0	0	0	0	0	0	0	0	0	0	0	0.00	0
56	0	0	0	0	0	0	0	0	0	0	0	0	0	0.00	0
60	0	0	0	0	0	0	0	0	0	0	0	0	0	0.00	0
61	0	0	0	0	0	0	0	0	0	0	0	0	0	0.00	0
63	0	0	0	0	0	0	0	0	0	0	0	0	0	0.00	0
68	0	0	0	0	0	0	0	0	0	0	0	0	0	0.00	0
82	0	0	0	0	0	0	0	0	0	0	0	0	0	0.00	0
84	0	0	0	0	0	0	0	0	0	0	0	0	0	0.00	0
88	0	0	0	0	0	0	0	0	0	0	0	0	0	0.00	0
89	0	0	0	0	0	0	0	0	0	0	0	0	0	0.00	0
91	0	0	0	0	0	0	0	0	0	0	0	0	0	0.00	0
94	0	0	0	0	0	0	0	0	0	0	0	0	0	0.00	0
97	0	0	0	0	0	0	0	0	0	0	0	0	0	0.00	0
99	0	0	0	0	0	0	0	0	0	0	0	0	0	0.00	0
104	0	0	0	0	0	0	0	0	0	0	0	0	0	0.00	0
108	0	0	0	0	0	0	0	0	0	0	0	0	0	0.00	0
109	0	0	0	0	0	0	0	0	0	0	0	0	0	0.00	0
111	0	0	0	0	0	0	0	0	0	0	0	0	0	0.00	0
114	0	0	0	0	0	0	0	0	0	0	0	0	0	0.00	0
115	0	0	0	0	0	0	0	0	0	0	0	0	0	0.00	0
120	0	0	0	0	0	0	0	0	0	0	0	0	0	0.00	0
121	0	0	0	0	0	0	0	0	0	0	0	0	0	0.00	0
130	0	0	0	0	0	0	0	0	0	0	0	0	0	0.00	0
134	0	0	0	0	0	0	0	0	0	0	0	0	0	0.00	0
136	0	0	0	0	0	0	0	0	0	0	0	0	0	0.00	0

137	0	0	0	0	0	0	0	0	0	0	0	0	0	0.00	0
141	0	0	0	0	0	0	0	0	0	0	0	0	0	0.00	0
142	0	0	0	0	0	0	0	0	0	0	0	0	0	0.00	0
143	0	0	0	0	0	0	0	0	0	0	0	0	0	0.00	0
145	0	0	0	0	0	0	0	0	0	0	0	0	0	0.00	0
146	0	0	0	0	0	0	0	0	0	0	0	0	0	0.00	0
152	0	0	0	0	0	0	0	0	0	0	0	0	0	0.00	0
153	0	0	0	0	0	0	0	0	0	0	0	0	0	0.00	0
156	0	0	0	0	0	0	0	0	0	0	0	0	0	0.00	0
157	0	0	0	0	0	0	0	0	0	0	0	0	0	0.00	0
158	0	0	0	0	0	0	0	0	0	0	0	0	0	0.00	0
161	0	0	0	0	0	0	0	0	0	0	0	0	0	0.00	0
Mean	0.38	0.7	0.5	0.6	0.3	0.2	0	0.2	0	0	0.1	0.7			
Sum	60	110	74	101	49	25	21	25	25	18	19	110			

885

886

Supplementary Table ST2. Covariates used in Equation 6. Comparison of the summary statistics of the mixed linear model with covariates of 1, 2 and 3 months before mosquito collection. * coefficient significant at 0.05 level.

Lag 1 month		
Covariates (scaled)	**Coefficient**	**Standard errors**
Air temperature	0.521*	0.227
Wet bulb temperature	-0.625*	0.226
Relative humidity	0.243*	0.098
Lag 2 months		
Covariates (scaled)	**Coefficient**	**Standard errors**
Air temperature	-0.014	0.247
Wet bulb temperature	-0.060	0.242
Relative humidity	0.072	0.105
Lag 3 months		
Covariates (scaled)	**Coefficient**	**Standard errors**
Air temperature	0.257	0.269
Wet bulb temperature	-0.270	0.264
Relative humidity	0.198	0.114

908

909

910

911

912

913 Supplementary table ST3. Moran curve parameters at each trap (last row for the general model).

Idtrap	λ_0, *field fertility*	*d*	α (degrees)
3	1.000	0.461	47.452
4	1.000	0.473	47.848
5	1.000	0.540	50.431
6	1.000	0.493	50.631
8	1.873	1.266	105.256
10	1.000	0.515	55.163
13	1.000	0.463	47.641
14	1.000	0.457	46.830
15	1.000	0.482	48.286
17	0.917	0.244	25.185
19	1.092	0.690	64.068
20	0.929	0.432	41.866
21	1.000	0.414	41.470
22	1.000	0.412	41.198
23	1.000	0.551	54.104
24	1.029	0.637	56.742
25	1.015	0.566	53.755
26	1.000	0.457	46.840
30	1.189	0.782	75.291
32	0.933	0.446	42.456
34	1.000	0.491	48.224
35	0.929	0.428	41.348

36	0.941	0.591	56.520
37	1.000	0.456	46.793
38	1.000	0.486	49.655
39	1.238	0.649	61.033
41	0.929	0.422	41.390
42	1.000	0.558	57.554
45	1.000	0.465	47.924
46	1.381	0.804	71.867
47	1.000	0.474	49.142
49	1.000	1.026	90.862
50	1.000	0.484	48.529
51	0.917	0.244	25.185
52	1.306	0.822	76.925
54	1.000	0.777	72.747
57	1.000	0.497	47.090
58	1.000	0.456	46.793
59	0.929	0.458	45.858
62	1.000	0.414	41.357
64	1.000	0.631	58.761
65	1.034	0.558	50.360
66	1.000	0.608	58.353
67	1.000	0.491	49.453
69	1.000	0.456	46.793
70	1.125	0.813	70.033
71	1.239	0.834	78.801

72	1.025	0.956	92.372
73	1.000	0.355	33.657
74	1.071	0.544	53.290
75	1.000	0.459	47.118
76	1.383	0.963	84.801
77	1.000	0.467	42.802
78	1.198	0.654	66.007
79	1.000	0.574	57.219
80	1.000	0.478	49.727
81	1.148	0.730	64.476
83	1.025	0.579	48.687
85	1.331	0.727	71.190
86	1.161	0.610	62.575
87	1.000	0.516	50.673
90	1.783	0.994	87.444
92	1.842	0.984	86.875
93	1.000	0.414	41.356
95	1.000	0.456	46.781
96	1.077	0.606	63.590
98	1.182	0.836	99.484
100	1.000	0.464	47.893
101	1.000	0.469	48.501
102	1.000	0.500	50.733
103	1.067	0.701	72.159
105	0.980	0.828	78.371

106	1.000	0.782	81.486
107	1.071	0.623	63.432
110	1.000	0.458	47.048
112	1.000	0.497	50.222
113	1.000	0.479	49.963
116	1.000	0.544	54.439
117	1.000	0.548	60.147
118	1.000	0.405	40.301
119	1.000	0.465	46.102
122	1.000	0.497	49.065
123	1.000	0.605	58.992
124	1.215	0.632	61.034
125	1.000	0.443	45.102
126	1.000	0.495	47.888
127	1.000	0.474	49.144
128	1.000	0.498	48.293
129	1.079	0.905	52.019
131	1.571	0.943	84.750
132	1.062	0.506	48.672
133	0.923	0.349	34.071
135	1.474	1.997	121.792
138	1.114	0.972	83.941
139	1.154	0.772	87.059
140	1.182	0.836	99.484
144	1.000	0.476	48.228

	147	1.076	0.642	63.393
	148	1.059	0.719	73.096
	149	1.062	0.536	52.543
	150	1.384	0.720	66.359
	151	1.054	0.760	66.147
	154	1.000	0.440	44.666
	160	1.024	1.550	113.296
General model		1.048	0.585	56.281

914

915

Supplementary Table ST4. Summary statistics for the negative binomial generalized linear model fitting the mosquito densities at time t+1 (Nt1). * coefficient significant at 0.05 level.

Fixed effect		
Covariates	**Coefficient**	**Standard errors**
Intercept	-1.176*	0.111
Nt (abundance)	-0.971*	0.046
Air temperature (scaled)	0.135	1.559
Wet bulb temperature (scaled)	-0.563	1.552
Relative humidity (scaled)	0.229	0.665
Random effects	**Variance**	**Standard deviation**
Trap ID	0.699	0.836

932

933 ## Supplementary Figure

934

IGR	*Real rho*	*Permuted rho min*	*Permuted rho max*	*Probability permuted rho*
Lag 0				
Exact points				
Intrinsic growth	0.89	-0.70	0.95	0.003
Abundance	0.89	-0.40	0.97	0.057
Lag 1				
Exact points				
Intrinsic growth	0.89	-0.30	0.89	0.000
Abundance	0.89	0.60	1.00	0.720
Lag 2				
Exact points				
Intrinsic growth	0.89	0.05	1.00	0.580
Abundance	0.89	0.30	1.00	0.080
Lag 3				
Exact points				
Intrinsic growth	0.89	0.50	1.00	0.870
Abundance	0.89	0.30	1.00	0.130

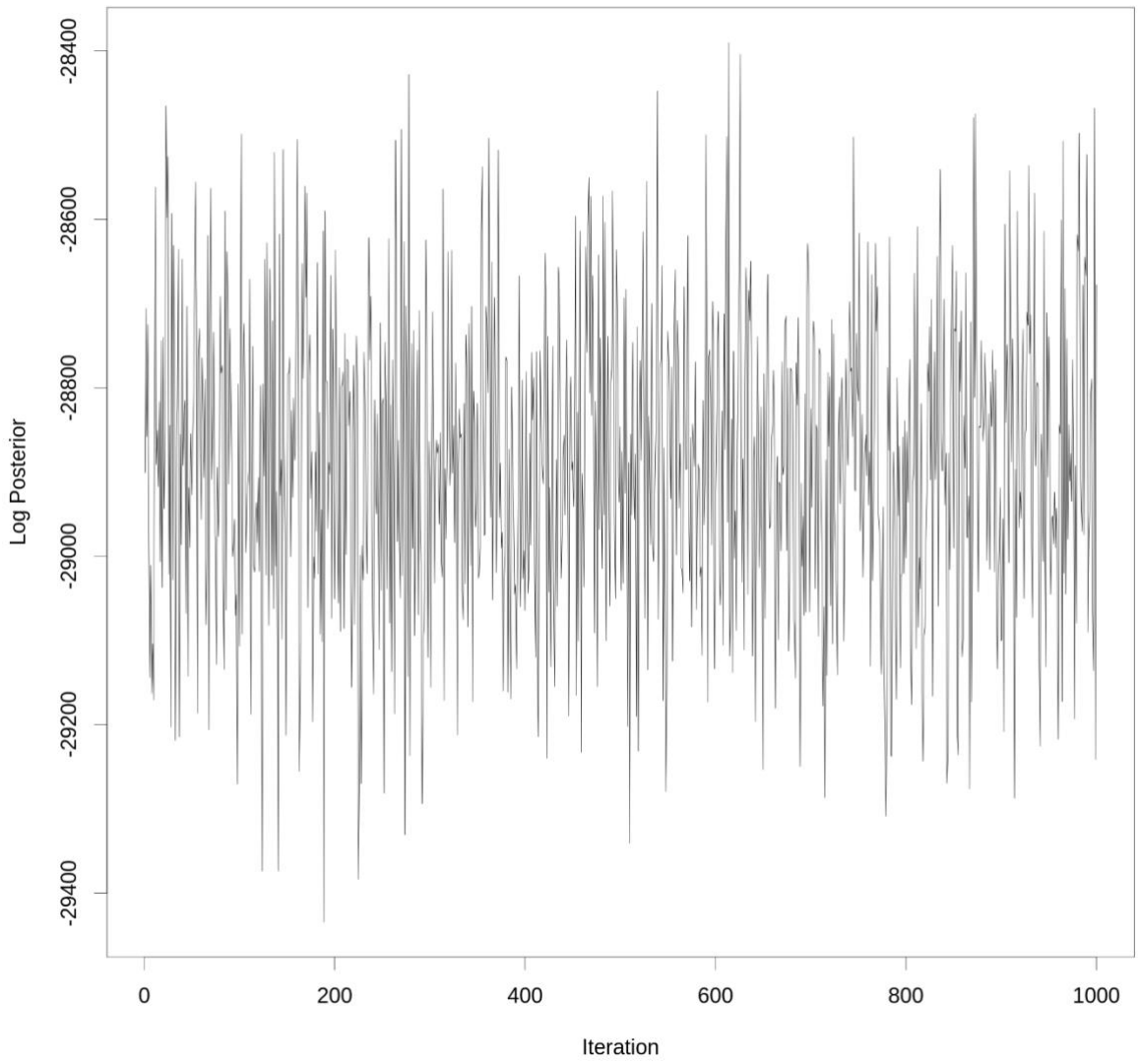

935

936 Supplementary Figure S1. Global convergence plot for the parameters of the spatio-temporal log-

937 Gaussian Cox model of dengue incidence with intrinsic growth rate as covariate.